

PL-TR-96-2311

MFD-96-TR-15649

**NETWORK IDENTIFICATION PERFORMANCE:  
(1) SIMULATIONS FOR THE MIDDLE  
EAST/NORTH AFRICA, AND (2) MAXIMUM  
LIKELIHOOD ESTIMATES OF TELESEISMIC  $m_b$   
FOR THE GSETT-3 PRIMARY NETWORK**

T. G. Barker

**Maxwell Technologies - Federal Division  
8888 Balboa Avenue  
San Diego, CA 92123-1506**

**September 1996**

**Scientific Report No. 1**

**Approved for public release; distribution unlimited.**



**DEPARTMENT OF ENERGY  
OFFICE OF NONPROLIFERATION AND  
NATIONAL SECURITY  
WASHINGTON, DC 20585**



**PHILLIPS LABORATORY  
Directorate of Geophysics  
AIR FORCE MATERIEL COMMAND  
HANSCOM AFB, MA 01731-3010**

**19970411 024**

**PROSECUTED BY REQUESTED 1**

SPONSORED BY  
Department of Energy  
Office of Non-Proliferation and National Security

MONITORED BY  
Phillips Laboratory  
CONTRACT No. F19628-95-C-0111

The views and conclusions contained in this document are those of the authors and should not be interpreted as representing the official policies, either express or implied, of the Air Force or U.S. Government.

This technical report has been reviewed and is approved for publication.



DELAINE R. REITER  
Contract Manager  
Earth Sciences Division



JAMES F. LEWKOWICZ  
Director  
Earth Sciences Division

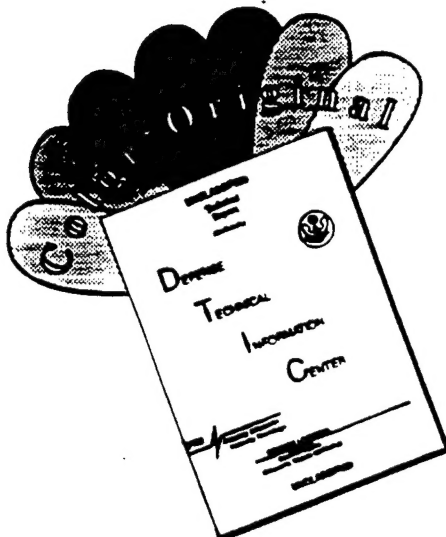
This report has been reviewed by the ESD Public Affairs Office (PA) and is releasable to the National Technical Information Service (NTIS).

Qualified requestors may obtain copies from the Defense Technical Information Center.  
All others should apply to the National Technical Information Service.

If your address has changed, or you wish to be removed from the mailing list, or if the addressee is no longer employed by your organization, please notify PL/IM, 29 Randolph Road, Hanscom AFB, MA 01731-3010. This will assist us in maintaining a current mailing list.

Do not return copies of this report unless contractual obligations or notices on a specific document requires that it be returned.

# **DISCLAIMER NOTICE**



**THIS DOCUMENT IS BEST  
QUALITY AVAILABLE. THE COPY  
FURNISHED TO DTIC CONTAINED  
A SIGNIFICANT NUMBER OF  
COLOR PAGES WHICH DO NOT  
REPRODUCE LEGIBLY ON BLACK  
AND WHITE MICROFICHE.**

REPORT DOCUMENTATION PAGE			Form Approved OMB No. 0704-0188
Public reporting burden for this collection of information is estimated to average 1 hour per response, including the time for reviewing instructions, searching existing data sources, gathering and maintaining the data needed, and completing and reviewing the collection of information. Send comments regarding this burden estimate or any other aspect of this collection of information, including suggestions for reducing this burden, to Washington Headquarters Services, Directorate for Information Operations and Reports, 1215 Jefferson Davis Highway, Suite 1204, Arlington VA 22202-4302, and to the Office of Management and Budget, Paperwork Reduction Project (0704-0188), Washington, DC 20503.			
1. AGENCY USE ONLY (Leave blank)	2. REPORT DATE	3. REPORT TYPE AND DATES COVERED	
	September 1996	Scientific Report No. 1	
4. TITLE AND SUBTITLE Network Identification Performance: (1) Simulations for the Middle East/North Africa and (2) Maximum Likelihood Estimates of Teleseismic $m_b$ for the GSETT-3 Primary Network		5. FUNDING NUMBERS Contract No.F19628-95-C-0111 PE 69120H PR DENN TA GM WU AC	
6. AUTHOR(S) Terrance G. Barker			
7. PERFORMING ORGANIZATION NAME(S) AND ADDRESS(ES) Maxwell Technologies - Federal Division 8888 Balboa Avenue San Diego, CA 92123-1506		8. PERFORMING ORGANIZATION REPORT NUMBER MFD-TR-96-15649	
9. SPONSORING/MONITORING AGENCY NAME(S) AND ADDRESS(ES) Phillips Laboratory 29 Randolph Road Hanscom Air Force Base, MA 01731-3010 Contract Manager: Delaine Reiter/GPE		10. SPONSORING/MONITORING AGENCY REPORT NUMBER PL-TR-96-2311	
11. SUPPLEMENTARY NOTES This research was sponsored by the Department of Energy, Office of Non-Proliferation and National Security, Washington, DC 20585			
12a. DISTRIBUTION/AVAILABILITY STATEMENT Approved for public release; distribution unlimited		12b. DISTRIBUTION CODE	
13. ABSTRACT (Maximum 200 words)  We have simulated the detection and identification performance of the current and proposed IMS seismic networks in the Middle East/North Africa. The identification performance of a network is strongly dependent upon regional source and propagation variability. However, knowledge of those variations allow one to estimate their effects and to know that in some areas certain discriminants can work and in other areas they do not. Data sources included published results on wave propagation in this region and incorporated analyses of data taken by Vernon, et al, (1996) in Saudi Arabia.  The maximum likelihood estimates of magnitude (Ringdal, 1976) was developed to improve measures of signal amplitudes which are below detection levels in some or all of the network As pointed out by Von Seggern and Rivers (1978), values of $m_b$ derived from arithmetic mean tend to have a positive bias, which may be eliminated by the use of maximum likelihood estimates. In this report, we simulate a suite of earthquakes recorded at the GSETT-3 Alpha network, and compare the $m_b$ is computed using the two methods with true values.			
14. SUBJECT TERMS seismology Monte Carlo simulations			15. NUMBER OF PAGES 32
seismic discrimination regional propagation			16. PRICE CODE
17. SECURITY CLASSIFICATION OF REPORT Unclassified	18. SECURITY CLASSIFICATION OF THIS PAGE Unclassified	19. SECURITY CLASSIFICATION OF ABSTRACT Unclassified	20. LIMITATION OF ABSTRACT SAR

**Unclassified**

**SECURITY CLASSIFICATION OF THIS PAGE**

**CLASSIFIED BY:**

**DECLASSIFY ON:**

**SECURITY CLASSIFICATION OF THIS PAGE**

**Unclassified**

## Table of Contents

<u>Section</u>	<u>Page</u>
1. Simulations for the Middle East/North Africa.....	1
1.1 Introduction.....	1
1.2 IGPP Data Set and Regional Properties .....	1
1.3 Noise Levels of Saudi Stations.....	7
1.4 Simulations of Detection and Identification Performance.....	7
2. Maximum Likelihood Estimates of Teleseismic $m_b$ for the GSETT-3 Primary (Alpha) Network .....	15
2.1. Introduction.....	15
2.2 Simulations.....	15
2.2.1. Source Properties.....	15
2.2.2 Propagation Parameters.....	15
2.2.3 GSETT-3 Primary Station Network.....	16
2.3 Results.....	17
3. References .....	23

## List of Illustrations

<u>Figure</u>		<u>Page</u>
1	The current IMS network and the area for which the simulations were done.....	2
2	The network used by Vernon, <i>et al.</i> (1996) (solid triangles) and the locations of earthquakes (open circles) analyzed for this study .....	3
3	Observed distribution of events with $m_b(+)$ and fit to the distribution(x).....	4
4	Grid of source and propagation parameters used in the simulations .....	5
5	Noise spectra for five Saudi stations on the same day (1995339), plus the low noise model proposed by Peterson (1993) .....	7
6	Proposed IMS seismic stations.....	8
7	Contours of $m_b$ detection thresholds for the current network.....	9
8	Contours of $m_b$ detection thresholds for the proposed IMS network.....	10
9	Contours of $m_b(Lg)$ detection thresholds for the proposed IMS network.....	11
10	Contours of $m_b(Lg)$ excitation levels $S_0$ .....	12
11	Contours of Lg/P ratio .....	12
12	Contours of fraction of events identified as earthquakes by the Lg/P discriminant at $m_b=3.5$ for the proposed IMS network.....	13
13	Contours of fraction of events identified as earthquakes by the Lg/P discriminant at $m_b=4.0$ for the proposed IMS network.....	14
14	Locations of stations (triangles) and events (circles) used in the simulations .....	17
15	Arithmetic mean $m_b$ (circles), ensemble average $m_b(x)$ and true $m_b$ (diamonds) are plotted versus log(moment).....	18
16	Maximum likelihood estimate $m_b$ (circles), ensemble average $m_b(x)$ and true $m_b$ (diamonds) are plotted versus log(moment).....	19
17	Arithmetic mean $m_b$ are plotted against maximum likelihood estimate $m_b$ .....	20
18	Incremental number of events versus $m_b^{mle}$ (circles) and $m_b^{am}$ (diamonds).....	21
19	Cumulative number of events versus $m_b^{mle}$ (circles) and $m_b^{am}$ (diamonds) and true $m_b$ (inverted triangles) .....	22

**Network Identification Performance:**  
**(1) Simulations for the Middle East/North Africa, and**  
**(2) Maximum Likelihood Estimates of Teleseismic  $m_b$  for the**  
**GSETT-3 Primary Network**

*Terrance G. Barker*

## **1. Simulations for the Middle East/North Africa**

### **1.1 Introduction**

We have simulated the detection and identification performance of the current and proposed IMS seismic networks in the Middle East/North Africa. Figure 1 shows a map of Africa and western Eurasia with the current IMS alpha stations and the area for which the simulations were done. The identification performance of a network is strongly dependent upon regional source and propagation variability. However, knowledge of those variations allow one to estimate their effects and to know that in some areas certain discriminants can work and in other areas they do not. Data sources included published results on wave propagation in this region and incorporated analyses of data taken by Vernon, *et al.* (1996) in Saudi Arabia.

### **1.2 IGPP Data Set and Regional Properties**

We recently received data collected by Vernon, *et al.* (1996) on the Arabian Shield. The data were provided to us by Frank Vernon. Using the larger events in their data set for which there were magnitudes reported in the IMS Reviewed Event Bulletin, we extracted parameters which we used to make simulations for this region. The stations in their array and the events we analyzed are plotted in Figure 2. The IMS coverage currently is quite sparse in this region, so their data represents an important increment in knowledge there. In addition, the data set allows us to infer noise levels directly for stations on the shield.

Before analyzing specific events in the dataset, we examined the entire origin file to infer an approximate  $m_b$  threshold for the region. If the probability of detection is a Gaussian distribution  $P(m_b; \mu, \sigma)$  with mean  $\mu$  and sigma  $\sigma$ , then we assume the observed distribution follows

$$N_{inc} = P(m_b; \mu, \sigma) N_{occ}(m_b),$$
$$\log(N_{occ}) = a - b \log m_b$$

We further assume that  $b=1$  and then fit the distribution of observed magnitudes, which were from IMS bulletins. Figure 3 shows the data and fit, with  $a=6.5$ ,  $\mu=4.5$  and  $\sigma=0.3$ .

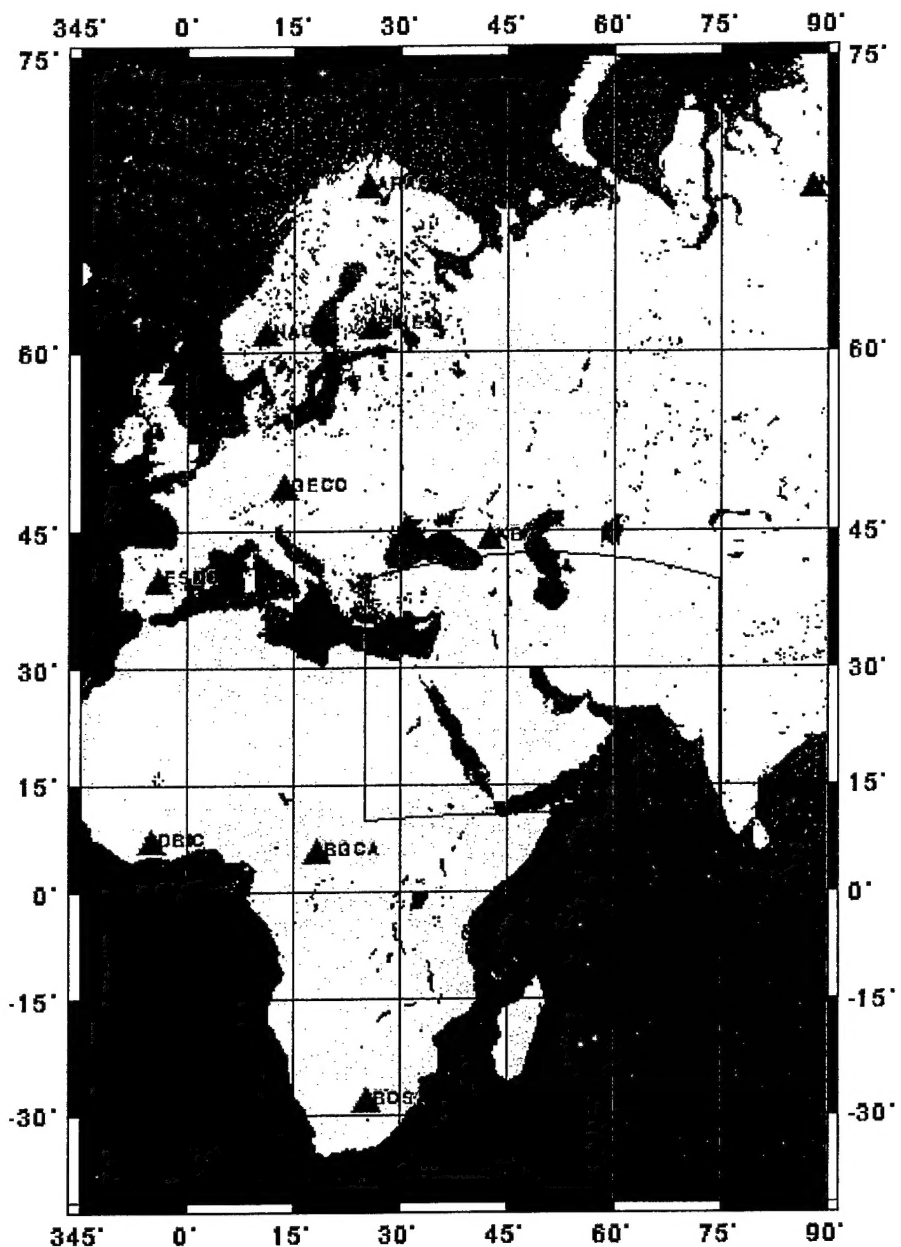


Figure 1. The current IMS network and the area for which the simulations were done.

Thus, the threshold for the IMS at the time these data were taken (late 1995 to early 1996) for the region as a whole was over  $m_b=4.5$ . By running simulations for that network we were able to set the scale factor in the P wave attenuation curves (effectively setting the relationship between moment and  $m_b$ ).

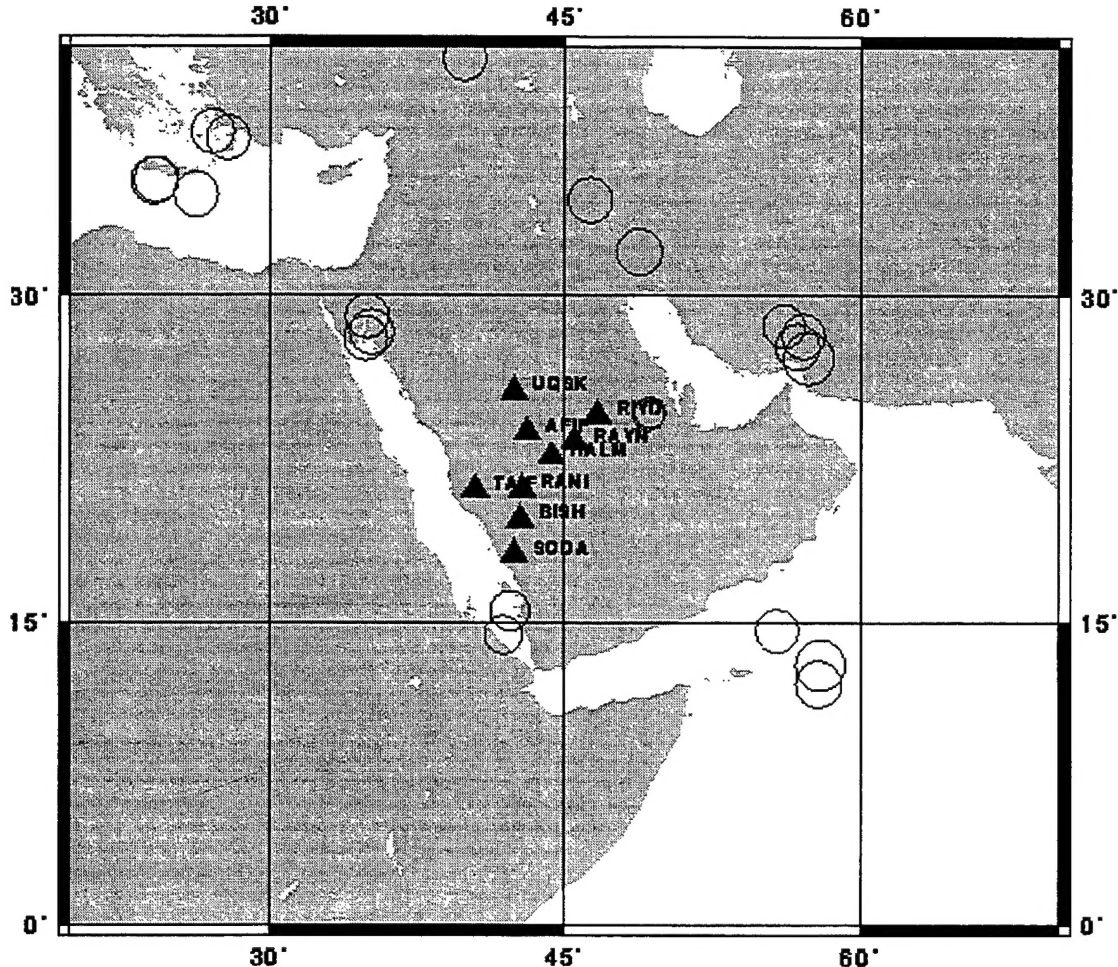


Figure 2. The network used by Vernon, *et al.* (1996) (solid triangles) and the locations of earthquakes (open circles) analyzed for this study.

Vernon, *et al.*, show that events in this region are very different in terms of their magnitude and relative amplitudes of regional phases. We selected events to represent five distinct areas, as suggested by Vernon, *et al.*, and measured time domain and spectral values. In order to source excitation levels, we calculated  $\log(Lg/P)$  values and log amplitudes corrected to  $m_b=4$  at a distance of 1000 km, relative to events in the NE Arabian Shield. That is,

$$\log A_{corr} = \log A_{obs}(mb, \Delta) + mb - 4 - 0.833 \log(\Delta / 1000) \quad (1)$$

It would be preferable to relate the values to a long period measure, but long period spectral values (computed by us) from some of the areas were poor and/or there were not  $M_s$  values from each of the regions. It would also be preferable to calculate sub-regional values of  $Q(f)$ , but this will be done by other institutions. Here, we assumed that values above 200 for  $Lg Q$  on the shield, near 200 off the shield and very low in the Red Sea. Table 1 shows the observed relative amplitudes.

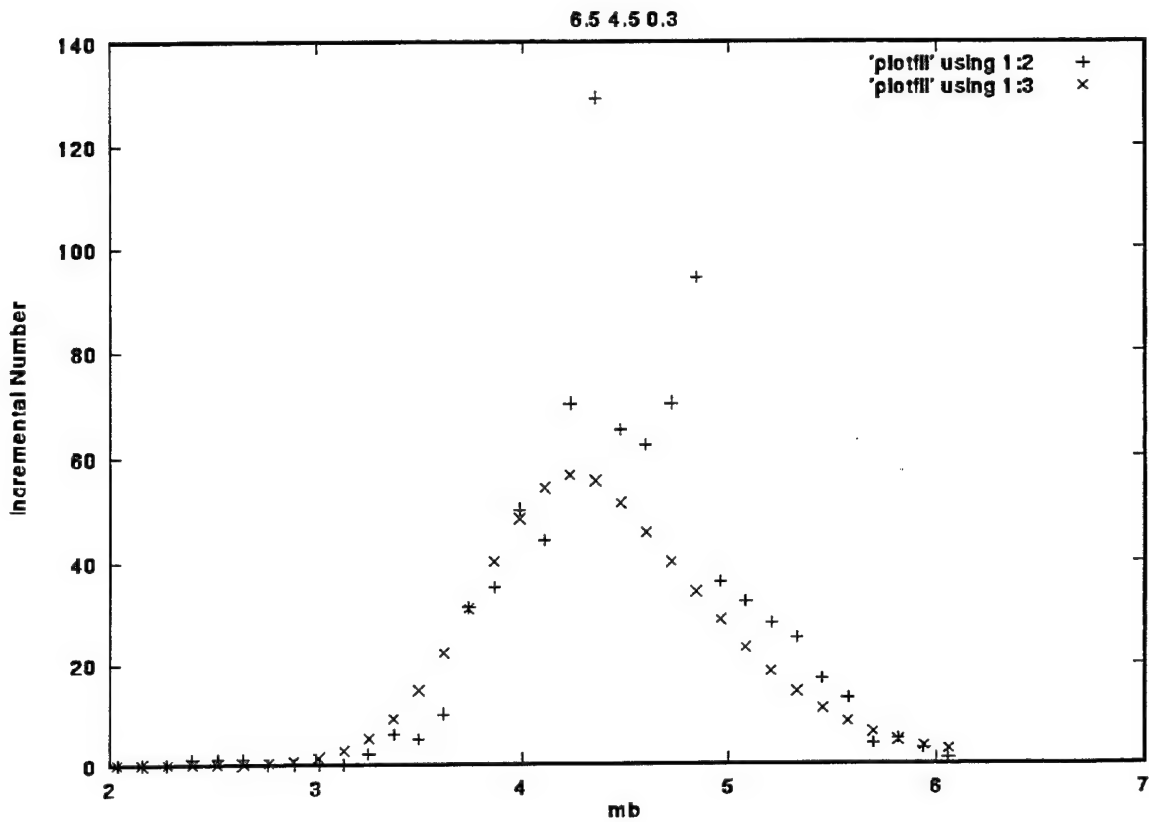


Figure 3: Observed distribution of events with  $m_b$ (+) and fit to the distribution(x).

Table 1. Observed Relative Amplitudes

Source region	$Lg/P$	$A_{corr}$ for Lg	$A_{corr}$ for Pn
NE Shield	0.3	0	0
S. Red Sea	1	-0.8	-1.5
Aqaba	2	0.5	-1.1
Zagros	-0.3	-1.5	-0.9
Arabian Sea	0.4	-1	-1

The study region was made into a grid that represents differences in source and propagation properties as reported by Vernon, *et al.* and summarized by Sweeney (1995). The values of Table 2 and the other studies were used to populate the grid, which is shown in Figure 4.

For each of the grid members, we used relative amplitudes of signals from the sub-regions to set the regional parameters. In Xnice, the spectral amplitude of a regional phase at distance  $\Delta$  has the form

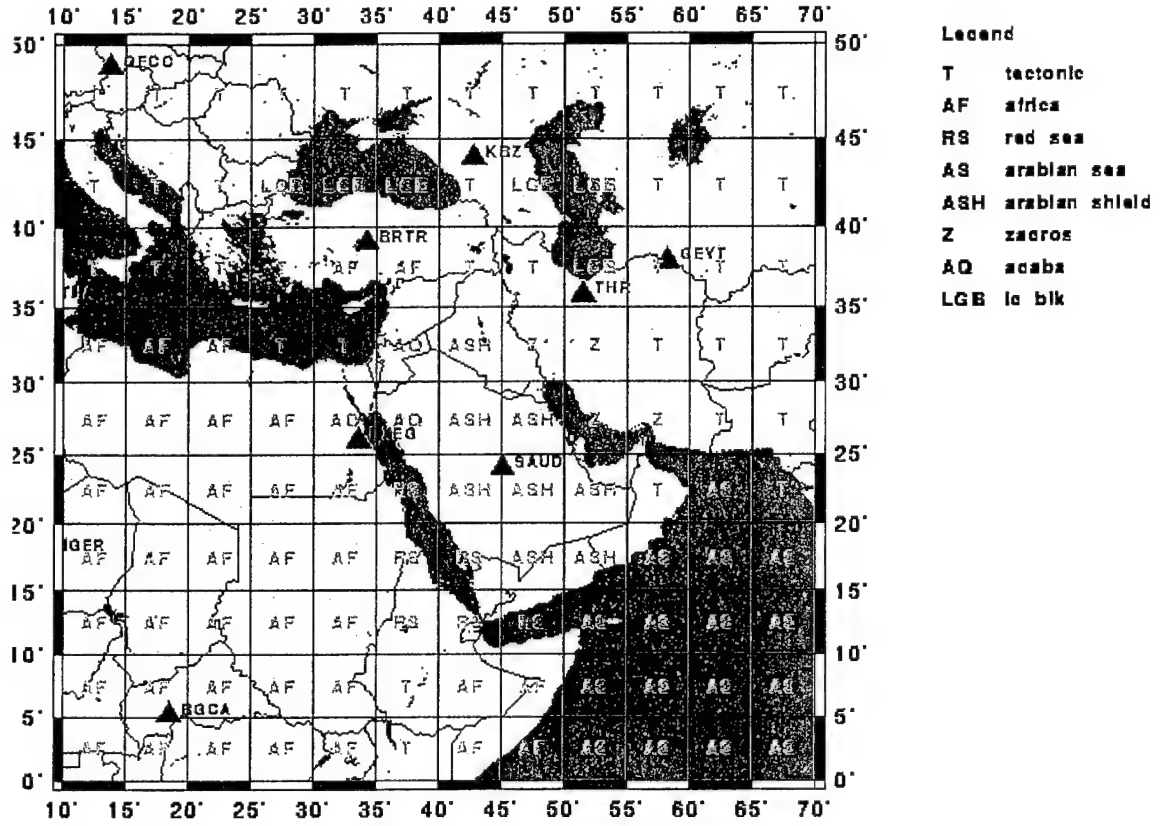


Figure 4. Grid of source and propagation parameters used in the simulations.

$$\begin{aligned} \log A_{eq} &= S_{eq}(f) + S_0 - 0.833\log(\Delta / \Delta_0) - 0.4342\gamma(\Delta - \Delta_0), \\ \log A_{ex} &= S_{ex}(f) + S_0 - 0.833\log(\Delta / \Delta_0) - 0.4342\gamma(\Delta - \Delta_0) + C_0^{\exp} + C_1^{\exp} \log(f), \end{aligned} \quad (2)$$

where  $S_{eq}(f)$  and  $S_{ex}(f)$  are the earthquake and explosion source spectra, and

$$\gamma = \pi f^{1-\eta} U_g^{-1} Q_0^{-1}.$$

Here,  $U_g$  is group velocity,  $Q_0$  is the quality factor at 1 Hz,  $\eta$  is the slope of the Q versus frequency relation,  $S_0$  is the source strength for unit moment, and  $C$  are the explosion relative source strength coefficients (see Barker, 1996 for details). The earthquakes generally occur in a narrow distance band (800 to 1100 km) from the network, so it was not possible to separate source and propagation factors from these data alone. We relied on the summary in Sweeney (1995) for Q values and used Baumgardt (1996) and Vernon, *et al.*, to deduce relative source strengths. There are no explosions in the data set, so we arbitrarily set  $C_0^{\exp}$  to zero for Lg and to one for Pg and Pn. Since we could not reliably estimate  $C_1^{\exp}$ , we did not examine discrimination performance based on explosion spectral slope. The parameters used in the simulations discussed here are summarized in Table 2.

Table 2. Regional Source and Propagation Parameters

africa						
Phase	$U_g$	$Q_0$	$\eta$	$S_0$	$C_0^{\text{exp}}$	$C_1^{\text{exp}}$
Lg	3500.	600.	0.39	-20.9	0.	-0.1
Pg	6000.	600.	0.39	-21.2	1.0	-0.5
Pn	8500.	600.	0.6	-21.2	0.8	-0.5
aqaba						
Phase	$U_g$	$Q_0$	$\eta$	$S_0$	$C_0^{\text{exp}}$	$C_1^{\text{exp}}$
Lg	3500.	200.	0.39	-20.4		-0.1
Pg	6000.	200.	0.39	-22.4	-21.9	-0.5
Pn	8500.	200.	0.6	-22.4	-21.9	-0.5
arabian_sea						
Phase	$U_g$	$Q_0$	$\eta$	$S_0$	$C_0^{\text{exp}}$	$C_1^{\text{exp}}$
Lg	3500.	200.	0.39	-21.9	0.0	-0.1
Pg	6000.	200.	0.39	-22.3	1.0	-0.5
Pn	8500.	200.	0.6	-22.3	1.0	-0.5
arabian_shield						
Phase	$U_g$	$Q_0$	$\eta$	$S_0$	$C_0^{\text{exp}}$	$C_1^{\text{exp}}$
Lg	3500.	300.	0.39	-20.9	0.2	-0.1
Pg	6000.	300.	0.39	-21.2	1.4	-0.5
Pn	8500.	300.	0.6	-21.2	0.8	-0.5
lg_blk						
Phase	$U_g$	$Q_0$	$\eta$	$S_0$	$C_0^{\text{exp}}$	$C_1^{\text{exp}}$
Lg	3500.	5.	0.45	-21.7	0.4	-1.1
Pg	6000.	10.	0.68	-22.7	0.8	-0.1
Pn	8500.	10.	0.8	-22.7	2.2	-0.1
red_sea						
Phase	$U_g$	$Q_0$	$\eta$	$S_0$	$C_0^{\text{exp}}$	$C_1^{\text{exp}}$
Lg	3500.	40.	0.45	-21.7	0.0	-1.1
Pg	6000.	40.	0.68	-22.7	1.0	-0.1
Pn	8500.	40.	0.8	-22.7	1.	-0.1
tectonic						
Phase	$U_g$	$Q_0$	$\eta$	$S_0$	$C_0^{\text{exp}}$	$C_1^{\text{exp}}$
Lg	3500.	671.	0.43	-21.2	0.3	-1.1
Pg	6000.	1000.	0.39	-21.5	1.4	-0.1
Pn	8500.	500.	0.6	-21.5	0.8	-0.1
zagros						
Phase	$U_g$	$Q_0$	$\eta$	$S_0$	$C_0^{\text{exp}}$	$C_1^{\text{exp}}$
Lg	3500.	200.	0.39	-22.6	0.0	-0.1
Pg	6000.	200.	0.39	-22.3	1.0	-0.5
Pn	8500.	200.	0.6	-22.3	1.0	-0.5

### 1.3 Noise Levels of Saudi Stations

For the simulations used here, we used time series from the IGPP data set to find noise levels for the proposed SAUD station. The Saudi stations are very quiet, as can be seen from Figure 5, which shows representative noise spectra for five stations on the same day, plus the low noise model proposed by Peterson (1993). The station noise levels are comparable to the low noise model, with the noise at station HALM significantly lower.

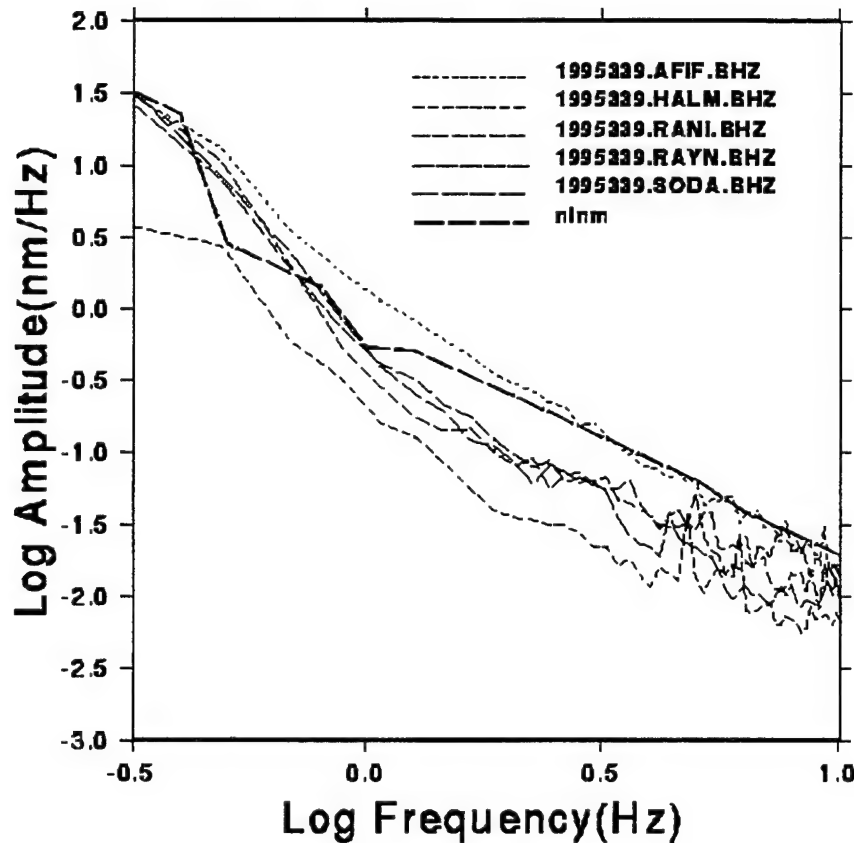


Figure 5. Noise spectra for five Saudi stations on the same day (1995339), plus the low noise model proposed by Peterson (1993).

### 1.4 Simulations of Detection and Identification Performance

The IMS network proposed by the Conference on Disarmament Experts working Group in August, 1995 is more dense in the Middle East (Figure 6) than that which is currently in place. In the following we compare estimates of the performance of the existing network with the proposed net. We begin with the detection thresholds.

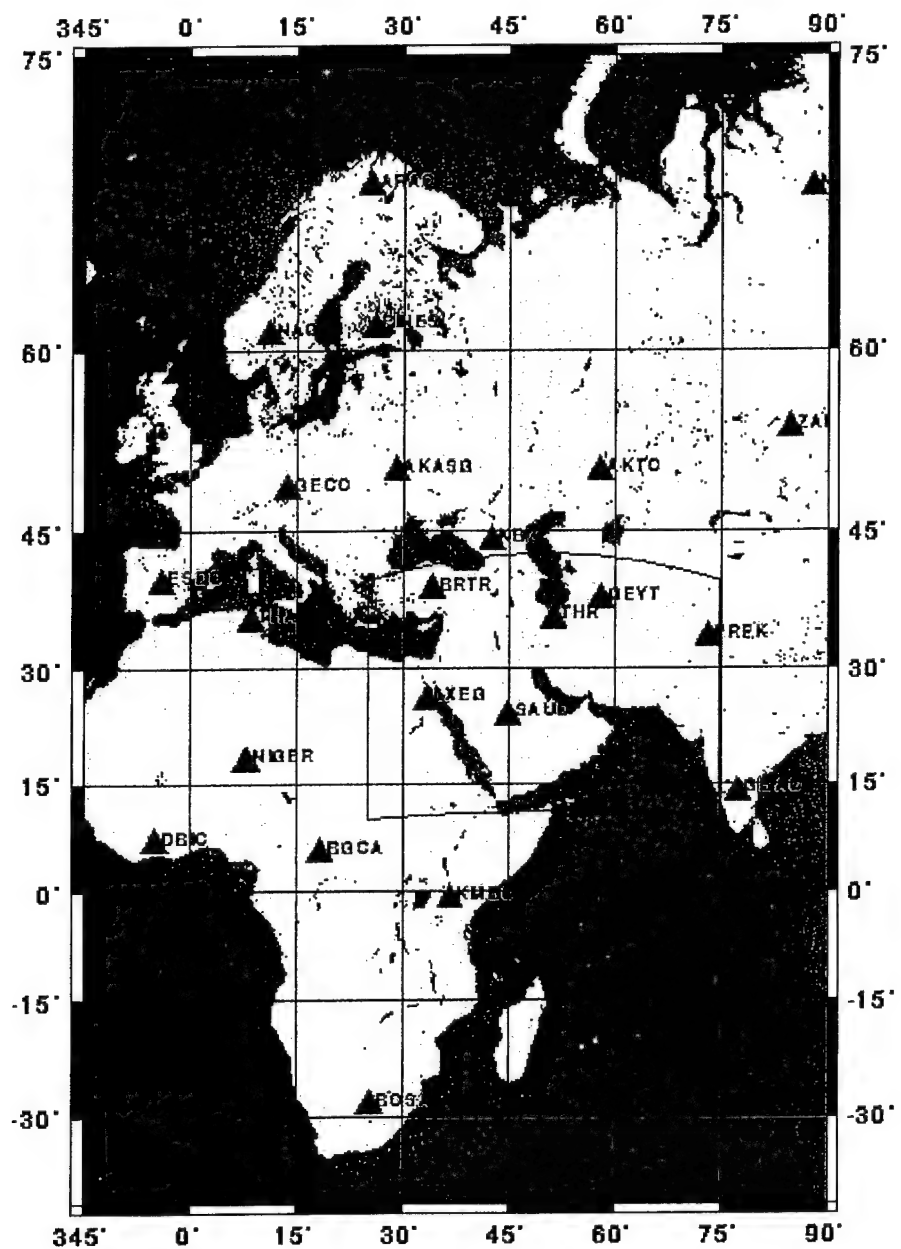


Figure 6. Proposed IMS seismic stations.

Contours of  $m_b$  detection thresholds for the current network are shown in Figure 7. By detection, we mean the criteria used in GSETT-3 and currently implemented on the IMS. The rules are based on a weighted sum of measurements (J. Carter, Center of Monitoring Research, personal communication):

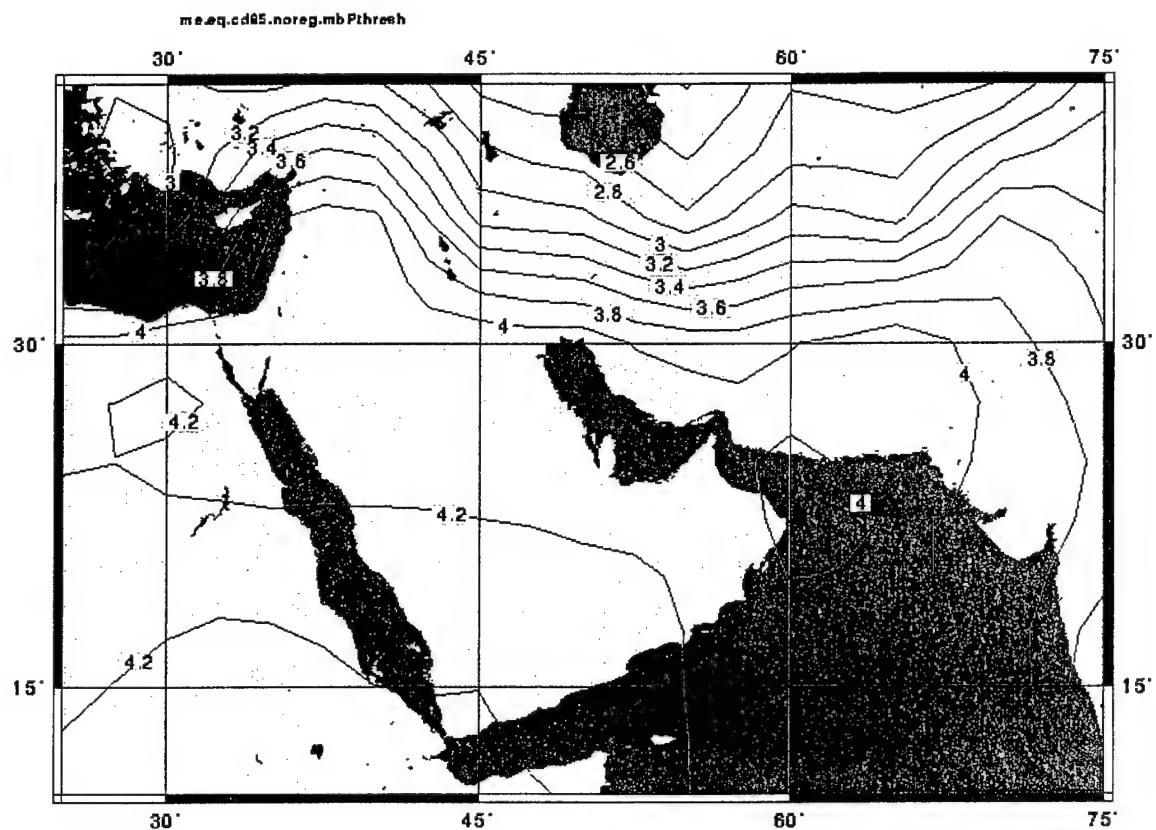


Figure 7. Contours of  $m_b$  detection thresholds for the current network.

Table 3. Weights for Measurements in Determining Detection Status

Primary Time	1.0
Secondary time	0.7
Array azimuth	0.4
Array slowness	0.4
Single station azimuth	0.2
Single station slowness	0.2

Here, "primary" refers to teleseismic P or regional Pg or Pn and secondary refers to teleseismic pP or S or regional Lg. All azimuths are determined from P, Pg or Pn. A sum is formed from the number of measurements which exceed the signal-to-noise ratio times their respective weights for the stations in the network. An event is considered detected if the sum exceeds 3.55. Thresholds in this figure and in the remainder of this report are 90% confidence values.

The thresholds decrease dramatically towards the NE as coverage improves. For events on the Arabian peninsula, detections are teleseismic (no stations are within the regional cutoff distance of 20 degrees). The detection thresholds for the proposed network are shown in Figure 8.

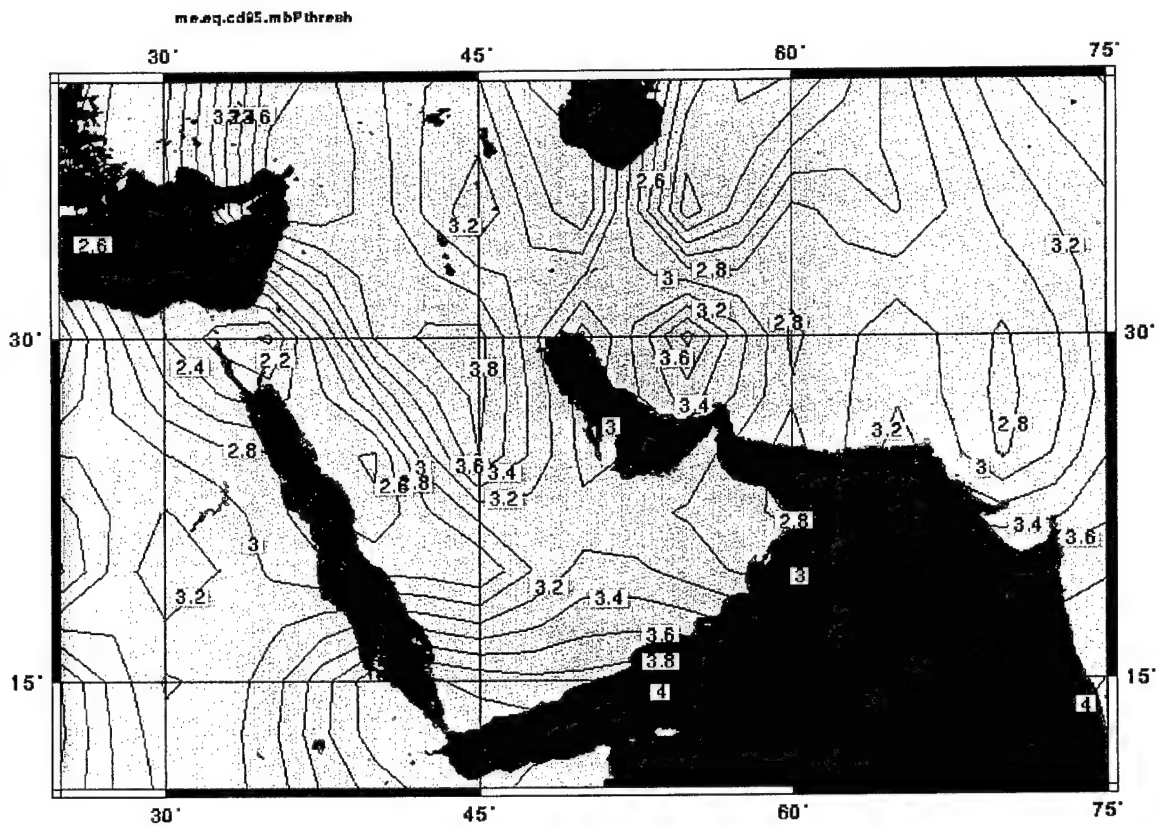


Figure 8. Contours of  $m_b$  detection thresholds for the proposed IMS network.

The additional stations lower the detection threshold substantially. Variability within the region is due to station geometry and variations in source strength and propagation parameters (Tables 1 and 2, Figure 4).

We turn now to identification performance. We note first that teleseismic discriminants are ineffective because events in this region (and the simulation) are typically shallow (<10 km). We did not model the  $M_s:m_b$  discriminant because we need accurate estimates of long-period noise for the networks, which we currently do not have. Thus, for events occurring on-shore, we must rely on regional discriminants for identification. Since there are no events detected (in the sense of the rules in Table 3) by the current IMS network in this region, discrimination cannot be done. On the other hand, the proposed network is capable of regional discrimination. We consider first the  $Lg/P$  discriminant. An event is considered identified as an earthquake if (1) the event satisfies the event detection criterion (Table 1), (2) both  $Lg$  and  $Pn$  or  $Pg$  exceed the signal-to-noise ratio at least 1 station, and (3) the  $Lg/P$  ratio exceeds a specified value. Figure 9 shows the contours of  $m_b(Lg)$  threshold.

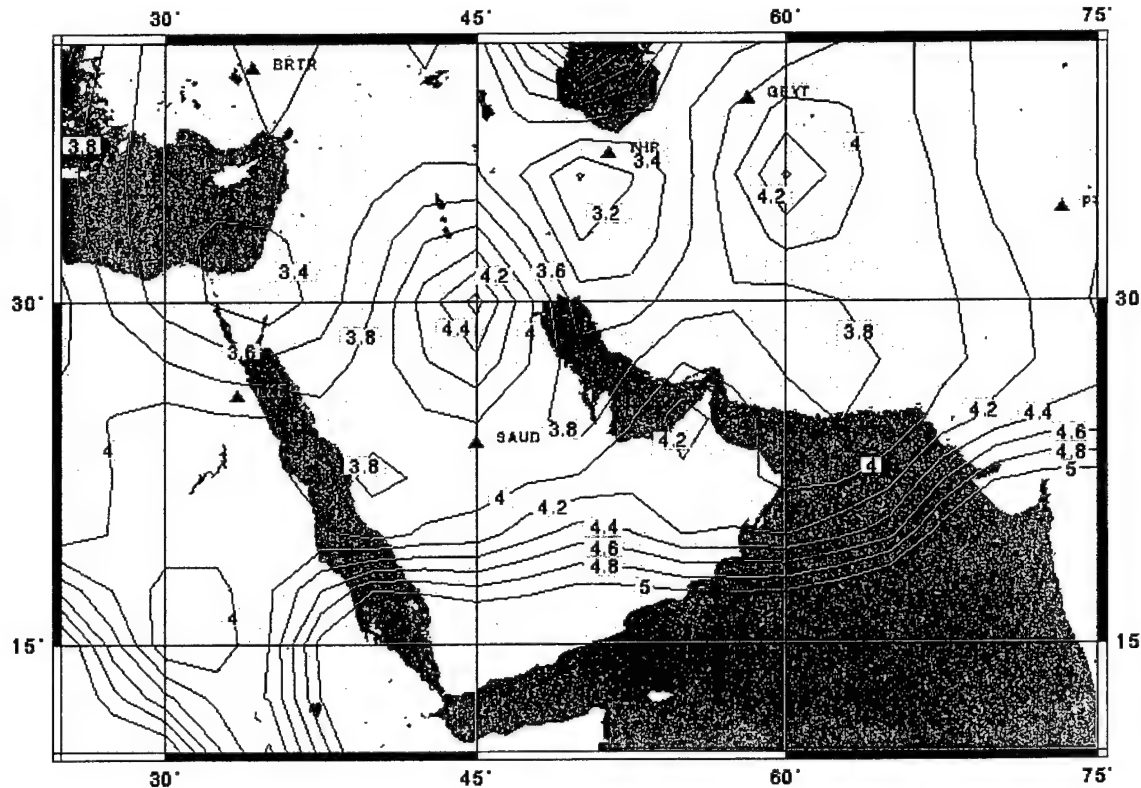


Figure 9. Contours of  $m_b(Lg)$  detection thresholds for the proposed IMS network.

Note that to the north of SAUD, the  $m_b(Lg)$  threshold increases locally. This is due primarily to the reduced excitation of Lg (see Table 1) towards the Zagros propagation grid zones. We can see the influence of the excitation levels  $S_0$  on  $m_b(Lg)$  from Figure 10, which shows contours those levels. In general, where the excitation is high, the threshold is low, and vice-versa. In addition to the detection of Lg, the Lg/P ratio must exceed a specified level. We show in Figure 10, contours of observed Lg/P, which are low towards the Zagros region, and high in the Gulf of Aqaba. We would thus expect from Figures 10 and 11 for the Lg/P ratio to identify earthquakes as such most successfully near the Gulf of Aqaba and least near the Zagros. Indeed this is the case, as seen in Figure 12 where we have plotted contours of the fraction of events with  $\log(Lg/P) > 0$  at  $m_b=3.5$ . The fractions are generally high where the observed Lg/P ratios are high, except in regions where the  $m_b(Lg)$  threshold is high, as in the NE part of the Arabian peninsula. The fraction of identified events is near one if we plot them at  $m_b=4.0$ , as shown in Figure 13. The values are still around 0.6 in the southern Red Sea, due to poor propagation and local values of  $\log(Lg/P)$  around 0.

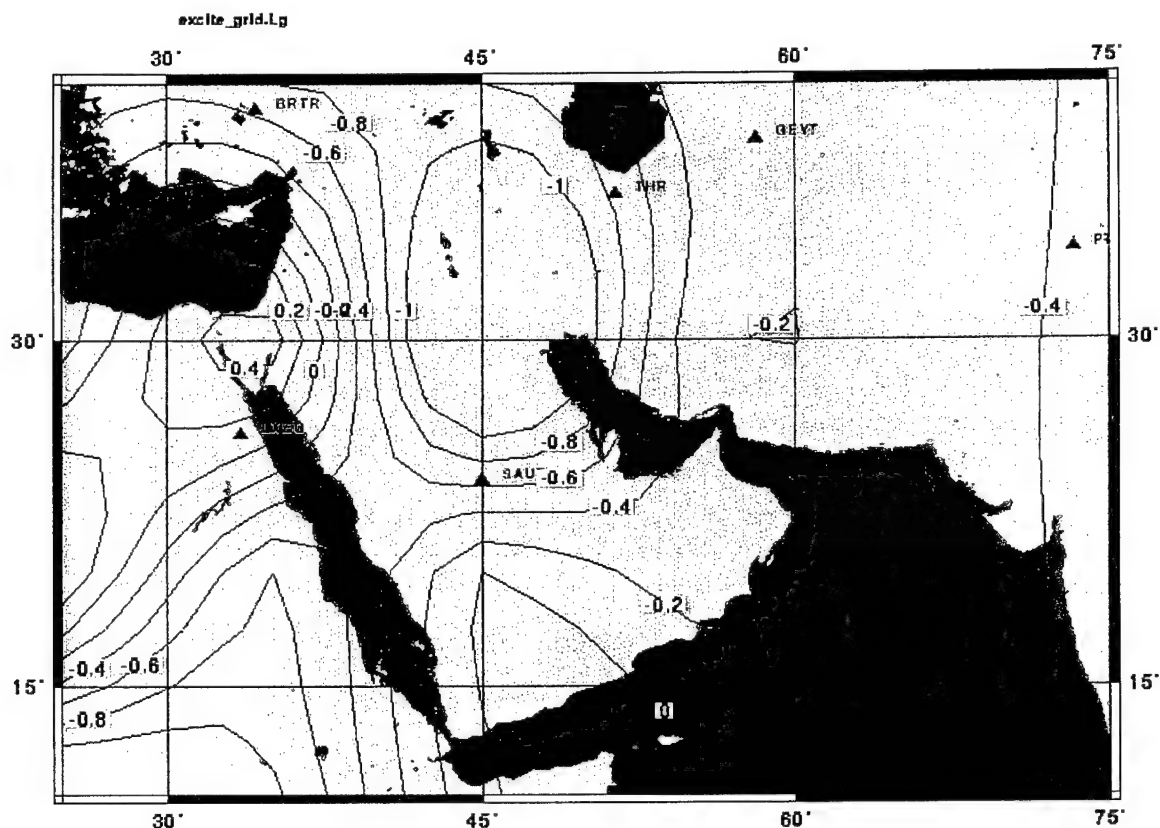


Figure 10. Contours of  $m_b(Lg)$  excitation levels  $S_0$ .

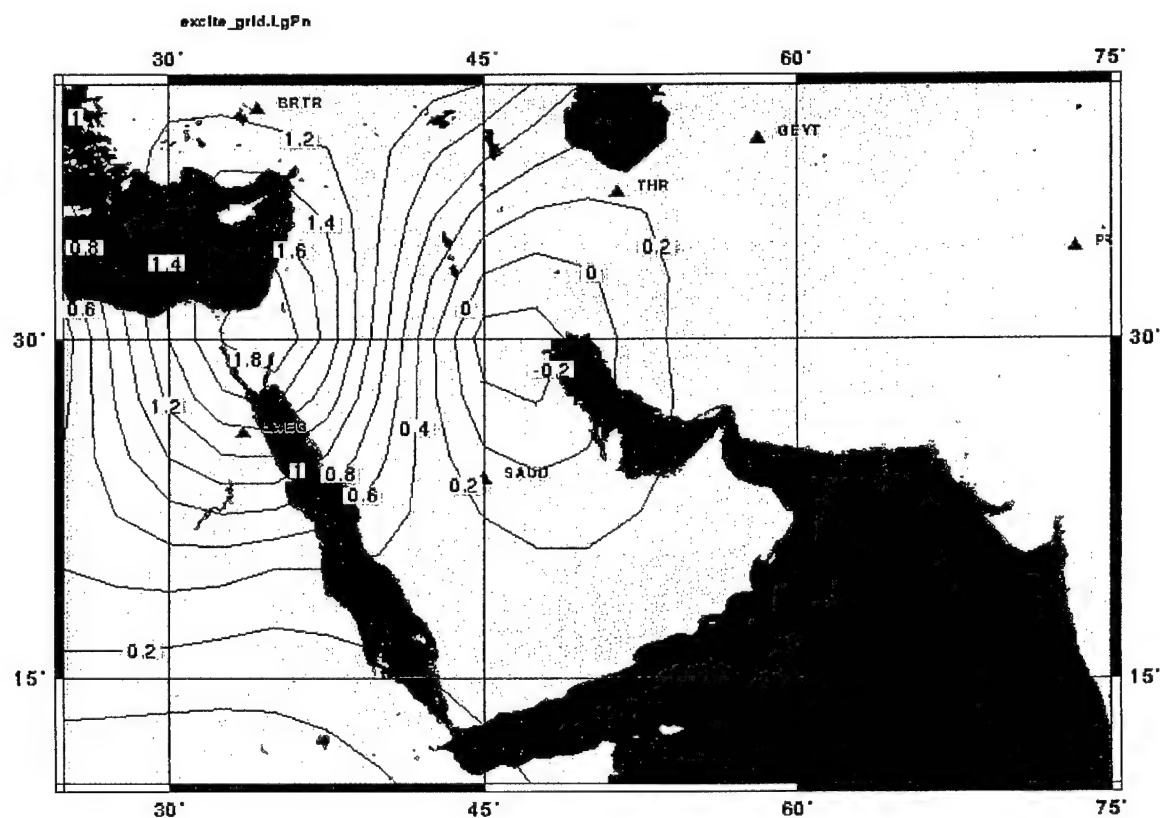


Figure 11. Contours of Lg/P ratio.

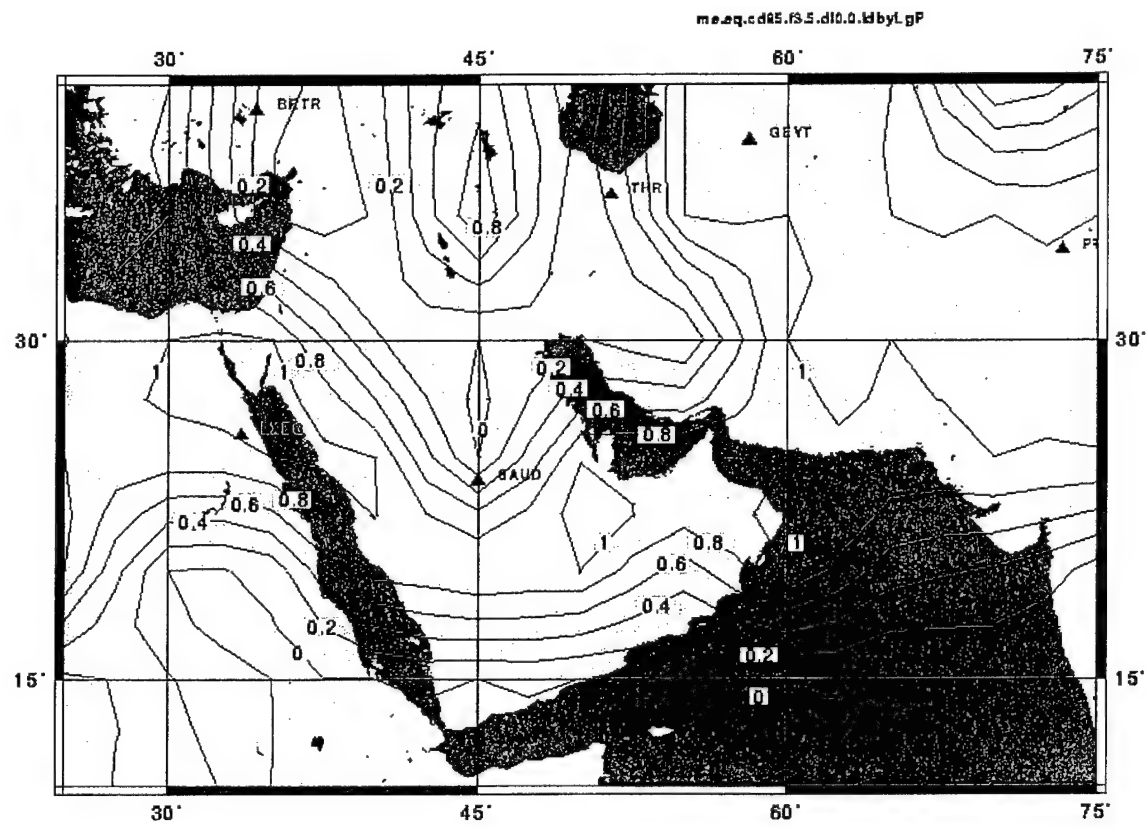


Figure 12. Contours of fraction of events identified as earthquakes by the Lg/P discriminant at  $m_b=3.5$  for the proposed IMS network. The decision line is  $\log(Lg/P) = 0.0$ .

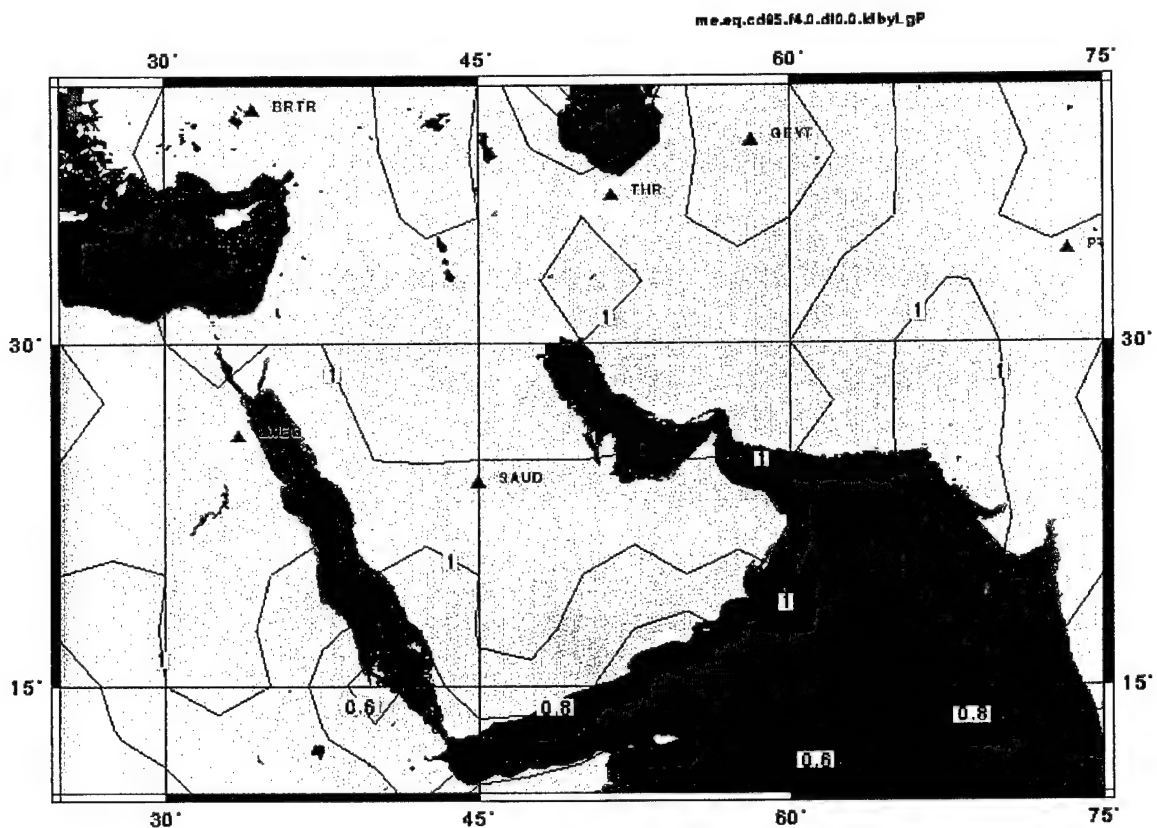


Figure 13. Contours of fraction of events identified as earthquakes by the Lg/P discriminant at  $m_b = 4.0$  for the proposed IMS network. The decision line is  $\log(Lg/P) = 0.0$ .

We do not currently have adequate excitation and propagation information at higher ( $>6$  Hz) to accurately simulate the regional (Lg or Pg/Pn) spectral slope discriminants. We can, however, address whether higher frequency signals could be detectable on the Arabian shield using noise spectra obtained from series preceding signals in Vernon's database. These stations are very quiet (Figure 5). Using the propagation parameters in Table 2 and a standard earthquake source model (Brune, 1970), we find that the higher frequency signals exceed the noise out to 10 Hz (even though signal power is decaying with frequency, the noise is decaying faster). That is, At locations where events can be detected at one Hz, they can generally be detected at ten Hz. If the station planned for Saudi Arabia is comparable to Vernon's stations, the spectral slope discriminants can be applied on the Arabian shield.

Each of the stations proposed in this region is very important to identification performance. Due to lack of coverage to the SE of SAUD (in the Arabian Sea), this station is essential for monitoring the Arabian shield and the Sanai peninsula. Without station LXEG, there are no regional detections in NE Africa and stations THR and BEYT are needed for regional detections south of the Caspian Sea.

## **2. Maximum Likelihood Estimates of Teleseismic $m_b$ for the GSETT-3 Primary (Alpha) Network**

### **2.1. Introduction**

The maximum likelihood estimates of magnitude (Ringdal, 1976) was developed to improve measures of signal amplitudes when are below detection levels in some or all of the network. As pointed out by Von Seggern and Rivers (1978), values of  $m_b$  derived from arithmetic mean tend to have a positive bias, which may be eliminated by the use of maximum likelihood estimates. In the following, we simulate a suite of earthquakes recorded at the GSETT-3 Alpha network, and compare the  $m_b$ 's computed using the two methods with true values.

### **2.2 Simulations**

The simulations described here use the Xnice program, described in detail in Barker, 1996. In the following, we specify parameters specific to this problem and refer the reader to that document for methods, models and other parameters.

#### **2.2.1. Source Properties**

So that a realistic geographic distribution of events is simulated, we extracted event locations from the Late Events Bulletin for 1993 to 1996 from the prototype IDC. This included about 20,000 events. Seismic moments were then distribution followed the rule

$$\begin{aligned} \log N_{cum} &= 2.85 - \log M_0, \\ \log M_0 &\geq 15, \end{aligned} \tag{3}$$

where  $N_{cum}$  is the cumulative number of events with moment  $\geq M_0$  (note that in Xnice a moment distribution is specified, rather than a magnitude). The stress drop were governed by log-normal distribution with a mean of 10 MPa (100 bars) and standard deviation of 5 MPa.

#### **2.2.2 Propagation Parameters**

Amplitude tables are from the Vieth and Claussen tables. Random errors in log amplitude of teleseismic P due to propagation followed a log-normal distribution with zero mean and 0.28 log-units standard deviation.

### 2.2.3 GSETT-3 Primary Station Network

The 41 stations used in this simulation, their location and mean log noise amplitude (microns) at 1 Hz are given the following table:

Station	Latitude	Longitude	Noise
AKT	50.434	58.018	-3.147
ARA0	69.535	25.506	-2.156
ASAR	-23.666	133.905	-2.774
BDFB	-15.633	-48.000	-2.899
BGCA	5.176	18.424	-3.349
BJT	40.018	116.168	-3.064
BOSA	-28.613	25.416	-2.726
CMAR	18.824	98.947	-2.920
CPUP	-26.331	-57.329	-2.919
DBIC	6.670	-4.856	-3.147
ESDC	39.675	-3.965	-2.751
FIA0	61.444	26.079	-2.488
GEC0	48.836	13.704	-3.147
HFS0	60.134	13.696	-2.814
KBZ	43.950	42.683	-3.147
LBNH	44.240	-71.930	-2.375
LOR	47.268	3.859	-2.618
LPAZ	-16.288	-68.131	-3.552
MAW	-67.604	62.871	-2.303
MBC	76.242	-119.360	-3.347
MIAR	34.546	-93.573	-2.868
MJAR	36.542	138.207	-2.891
NAO	61.040	11.215	-2.450
NPO	64.771	-146.886	-2.007
NRI	69.400	88.000	-3.179
PDAR	42.780	-109.560	-3.315
PDY	59.600	112.500	-3.073
PFCA	33.610	-116.460	-3.005
PLCA	-40.731	-70.550	-2.955
SCHQ	54.817	-66.783	-2.735
SPITS	78.180	16.370	-1.583
STKA	-31.882	141.592	-2.813
TXAR	29.334	-103.667	-3.243
ULM	50.250	-95.875	-3.015
VNDA	-77.519	161.846	-2.780
WALA	49.056	-113.911	-2.983
WHY	60.695	-134.967	-2.840
WOOL	-31.073	121.678	-2.919
WRA	-19.944	134.341	-3.020
YKA	62.493	-114.605	-3.433
ZAL	53.940	84.805	-3.463

The GSETT-3 Primary network of stations has a wide range of short-period noise levels ranging from a high of -1.6 (0.025 microns) to low values of -3.5 (0.003 microns).

### 2.3 Results

Figure 14 shows the locations of stations and events used in the simulations. In Figure 15, we have plotted arithmetic mean  $m_b$ 's ( $m_b^{am}$ ) versus  $\log M_0$ . Only those events which meet the GSE detection criteria are included. Also plotted in this figure is the ensemble average of the values of  $m_b$  within 0.125 of the plotted  $\log M_0$  (the averages are indicated by x's). A third set of values on the figure are the values of  $m_b$  when there is no propagation variation or ground noise and no statistical variation in the stress drop. We refer to these values as the "true" values. The curvature is due to the change in corner frequency with moment. We see that  $m_b^{am}$  exceed the true values by about 0.5 at the lowest magnitudes and approach the true value at higher  $m_b$ . Figure 16 shows a comparable plot for maximum likelihood estimated  $m_b$  ( $m_b^{mle}$ ). The values of  $m_b^{mle}$  are quite close to the true values across the magnitude range.  $m_b^{am}$  and  $m_b^{mle}$  are plotted against each other in Figure 17, which shows that the  $m_b^{am}$  exceed the  $m_b^{mle}$ , in agreement with Von Seggern and Rivers (1978).

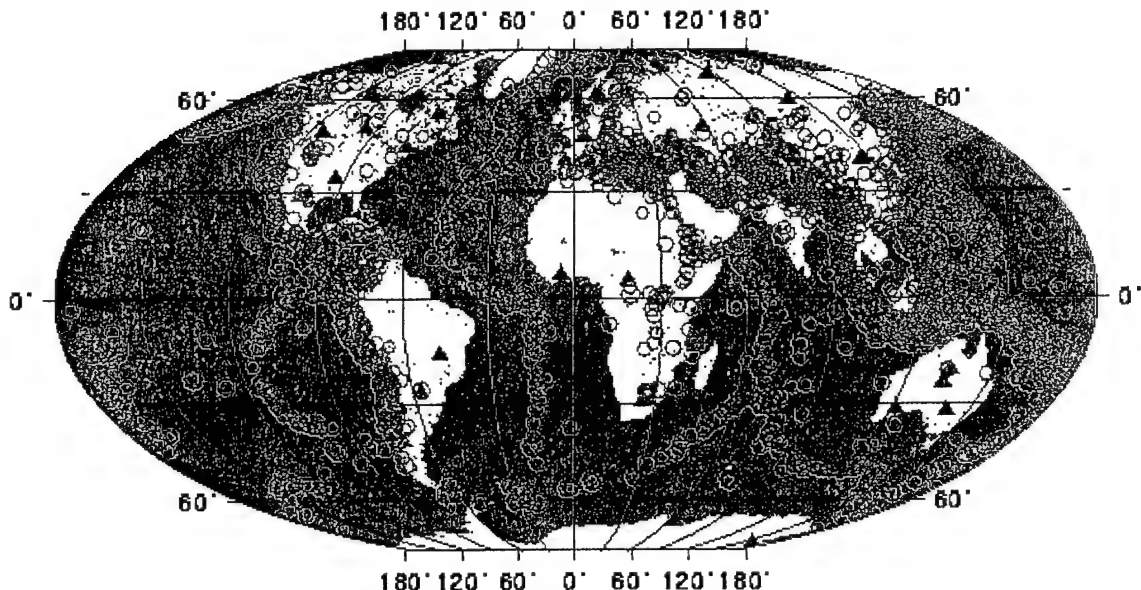


Figure 14. Locations of stations (triangles) and events (circles) used in the simulations.

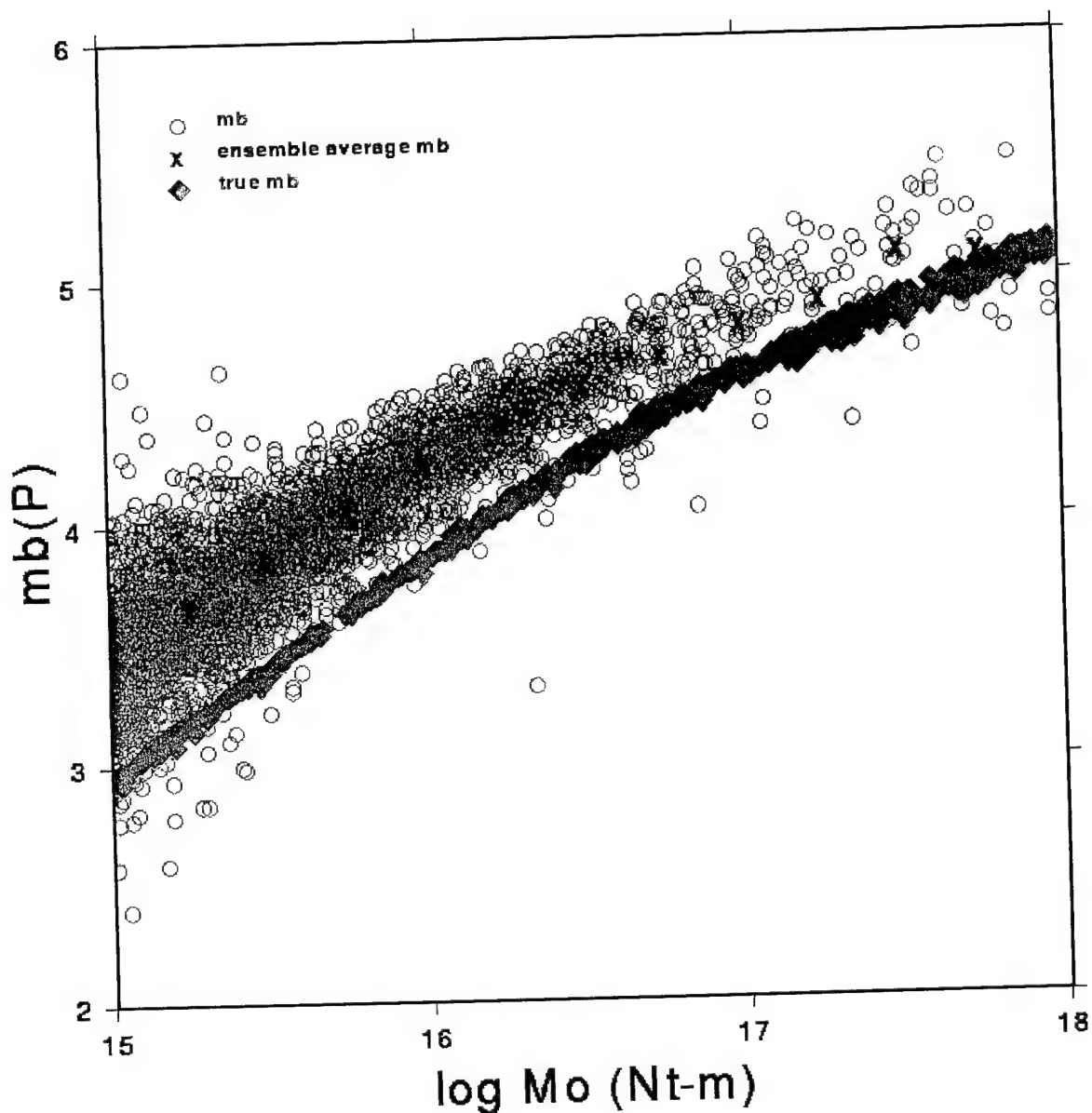


Figure 15. Arithmetic mean  $m_b$  (circles), ensemble average  $m_b$  (x) and true  $m_b$  (diamonds) are plotted versus  $\log(\text{moment})$ .

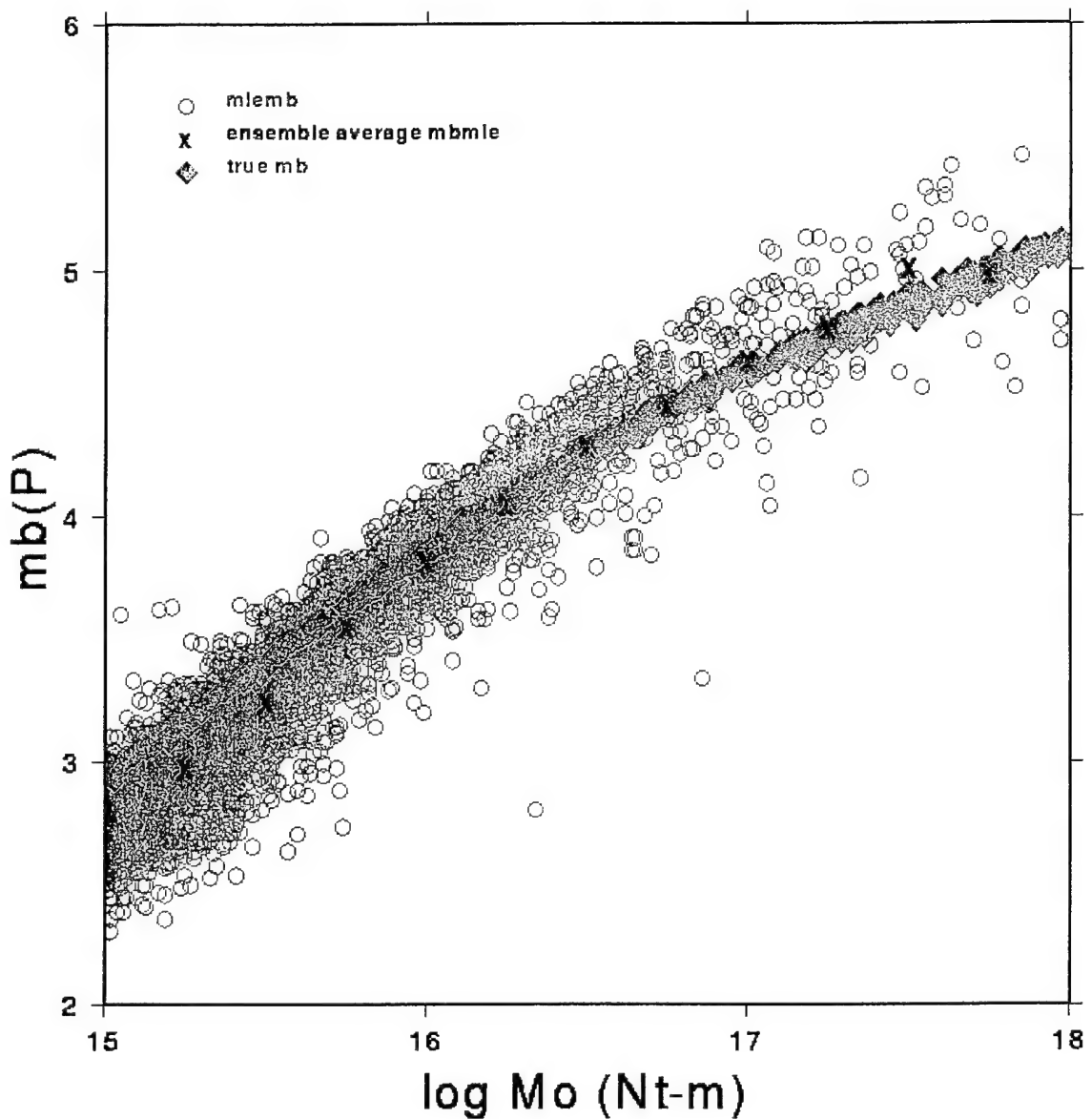


Figure 16. Maximum likelihood estimate  $m_b$  (circles), ensemble average  $m_b$  (x) and true  $m_b$  (diamonds) are plotted versus  $\log(\text{moment})$ .

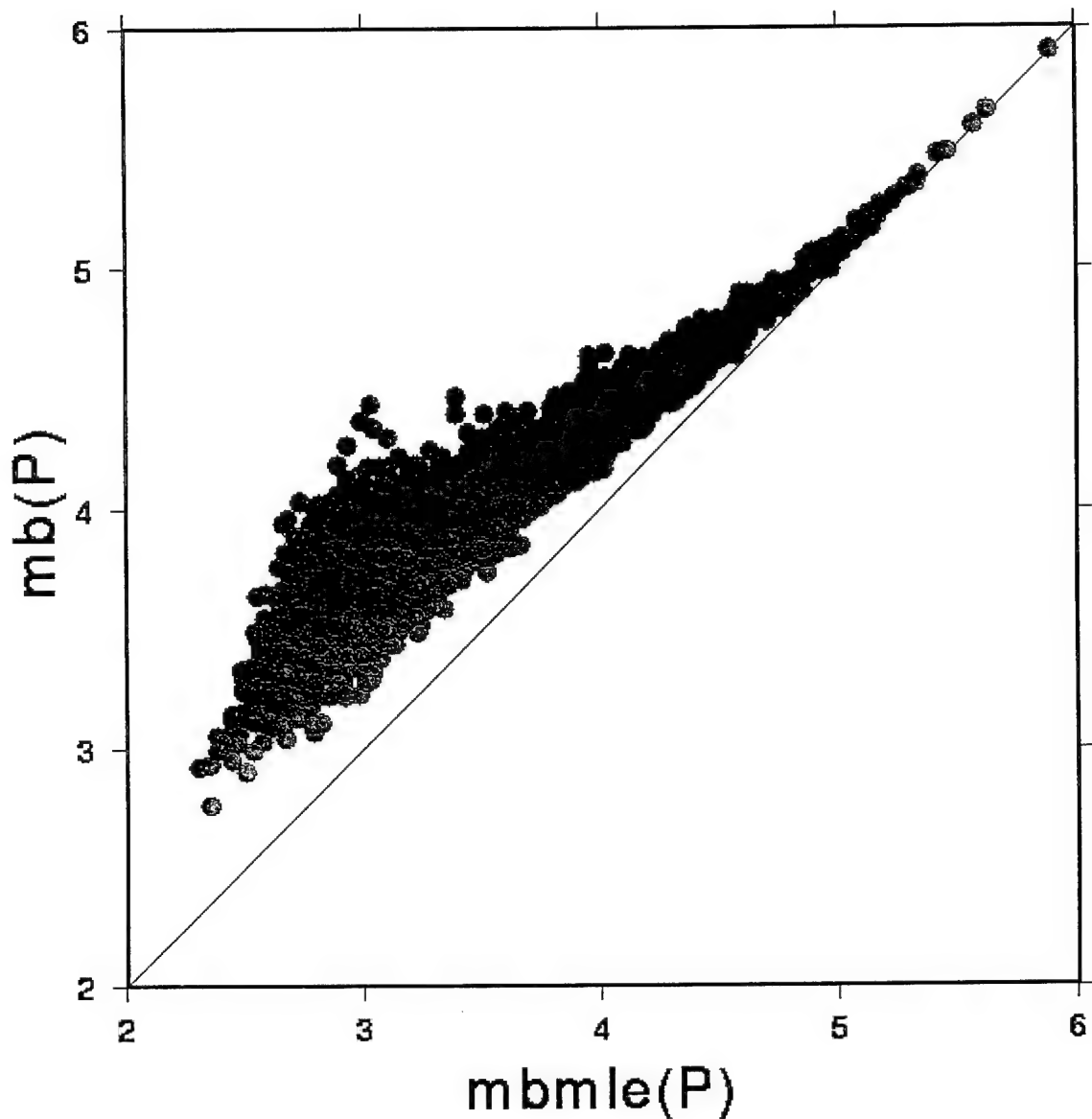


Figure 17. Arithmetic mean  $m_b$  are plotted against maximum likelihood estimate  $m_b$ .

The incremental number of events versus  $m_b^{mle}$  and  $m_b^{am}$  are shown in Figure 18. In each case the values are normalized by the total number of events detected. The peak number of events for  $m_b^{mle}$  occurs at a lower value than  $m_b^{am}$ , indicating an apparent lower detection threshold for  $m_b^{mle}$ . The cumulative numbers (number with values greater than  $m_b$ ) are shown in Figure 19. Also shown on this figure are the true values. The slope of the  $m_b^{mle}$  distribution at high magnitudes (from which a "b value" would be measured) has about the same value as the slope of the true values, while the  $m_b^{am}$  distribution has a greater slope. Note that the slope is greater than one (the slope of the log moment distribution above) due to corner frequency effects.

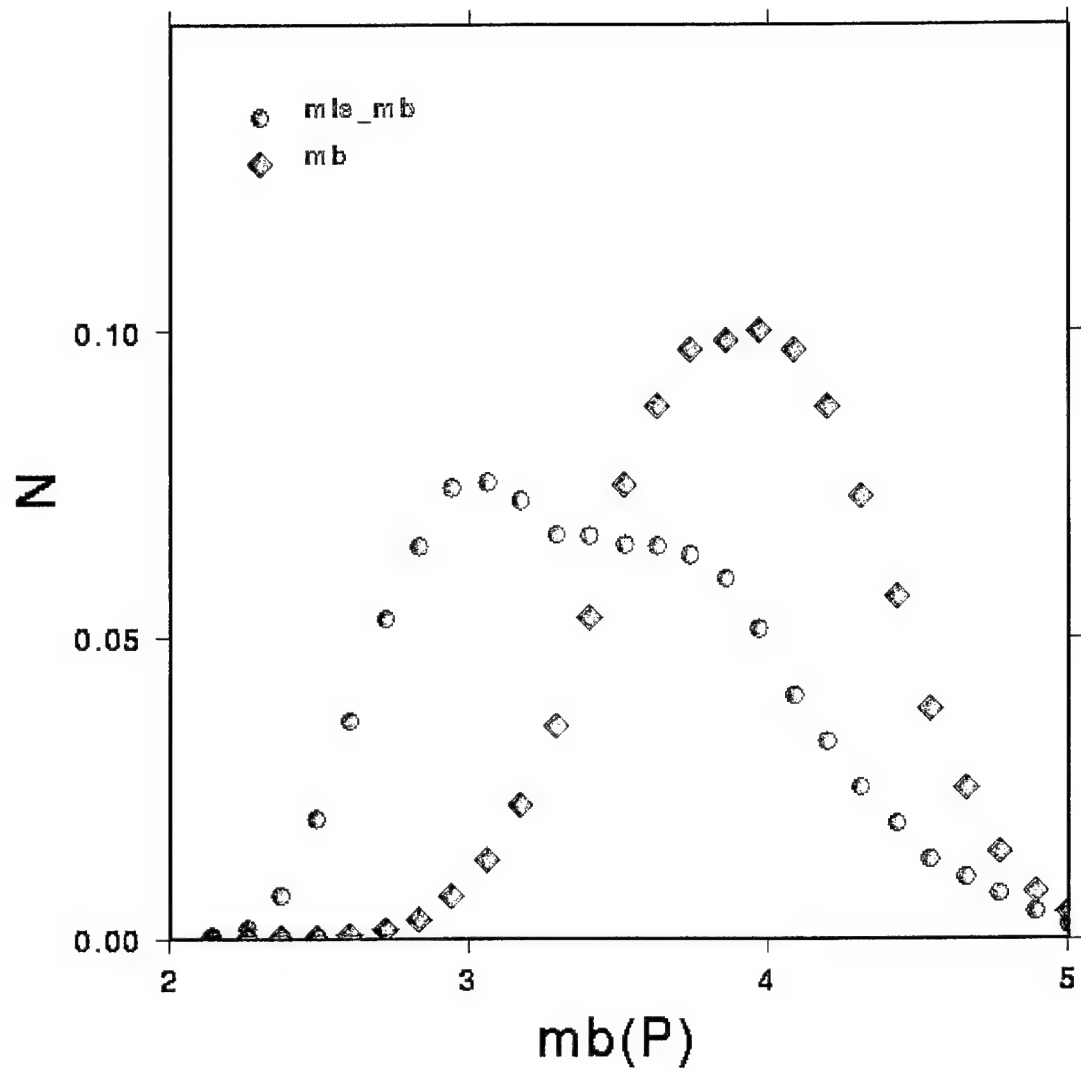


Figure 18. Incremental number of events versus  $m_b^{mle}$  (circles) and  $m_b^{am}$  (diamonds).

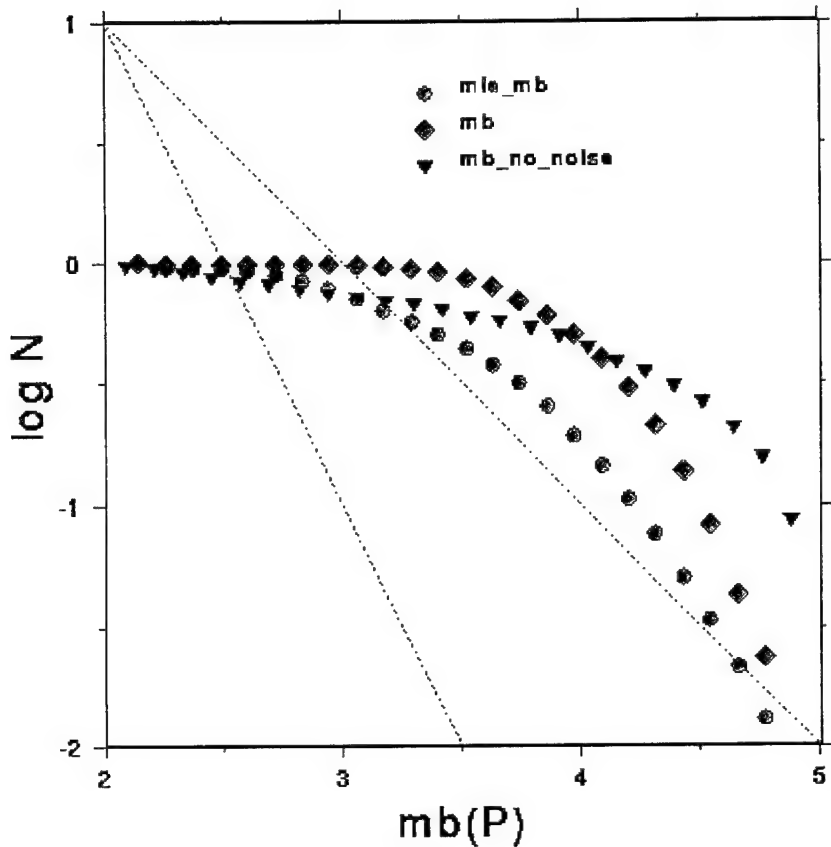


Figure 19. Cumulative number of events versus  $m_b^{mle}$  (circles) and  $m_b^{am}$  (diamonds) and true  $m_b$  (inverted triangles). Straight dashed lines have slopes of -1 and -2.

These results indicate that replacement of  $m_b^{am}$  with  $m_b^{mle}$  as the network  $m_b$  values in future bulletins will reduce magnitude bias at low magnitudes and decrease the slope of the cumulative distribution of events versus  $m_b$  in accordance with conventional wisdom.

### **3. References**

- Barker, T. G. (1996), "Xnice: A System for Assessing Network Identification Performance," S-CUBED Scientific Report No. 2 to Phillips Laboratory, PL-TR-96-2087.
- Baumgardt, D. R. (1996), "Characterization of Regional-Phase Propagation and Seismic Discriminants for the Middle East," *Proceedings of the 18<sup>th</sup> Annual Seismic Research Symposium on Monitoring a Comprehensive Test Ban Treaty*, edited by J. F. Lewkowicz, J. M. McPhetres and D. T. Reiter, Annapolis MD, PL-TR-96-2153, ADA313692.
- Peterson, J. (1993), "Observations and Modeling of Seismic Background Noise," U.S.G.S. Open-File Report 93-322.
- Sweeney, J. J. (1995), "Preliminary Maps of Crustal thickness and Regional Seismic Phases for the Middle East and North Africa," Lawrence Livermore National Laboratory Report UCRL-ID-122080.
- Ringdal, F. (1976), "Maximum Likelihood Estimation of Seismic Magnitude," *Bull. Seism. Soc. Am.*, **66**(3), 789-802.
- Vernon, F. R., R. J. Mellors, J. Berger, A. M. Al-Amri, and J. Zollweg, (1996), "Initial Results from the Deployment of Broadband Seismometers in the Saudi Arabian Shield," *Proceedings of the 18<sup>th</sup> Annual Seismic Research Symposium on Monitoring a Comprehensive Test Ban Treaty*, edited by J. F. Lewkowicz, J. M. McPhetres and D. T. Reiter, Annapolis MD, PL-TR-96-2153, ADA313692.
- Von Seggern, D. and D. W. Rivers (1978), "Comments on the Use of Truncated Distribution Theory for Improved Magnitude Estimation," *Bull. Seism. Soc. Am.*, **68**(5), 1543-1546.

THOMAS AHRENS  
SEISMOLOGICAL LABORATORY 252-21  
CALIFORNIA INSTITUTE OF TECHNOLOGY  
PASADENA, CA 91125

RALPH ALEWINE  
NTPO  
1901 N. MOORE STREET, SUITE 609  
ARLINGTON, VA 22209

SHELTON ALEXANDER  
PENNSYLVANIA STATE UNIVERSITY  
DEPARTMENT OF GEOSCIENCES  
537 DEIKE BUILDING  
UNIVERSITY PARK, PA 16801

MUAWIA BARAZANGI  
INSTITUTE FOR THE STUDY OF THE CONTINENTS  
3126 SNEE HALL  
CORNELL UNIVERSITY  
ITHACA, NY 14853

RICHARD BARDZELL  
ACIS  
DCI/ACIS  
WASHINGTON, DC 20505

T.G. BARKER  
MAXWELL TECHNOLOGIES  
P.O. BOX 23558  
SAN DIEGO, CA 92123

DOUGLAS BAUMGARDT  
ENSCO INC.  
5400 PORT ROYAL ROAD  
SPRINGFIELD, VA 22151

ATHERON J. BENNETT  
MAXWELL TECHNOLOGIES  
11800 SUNRISE VALLEY DRIVE SUITE 1212  
RESTON, VA 22091

WILLIAM BENSON  
NAS/COS  
ROOM HA372  
2001 WISCONSIN AVE. NW  
WASHINGTON, DC 20007

JONATHAN BERGER  
UNIVERSITY OF CA, SAN DIEGO  
SCRIPPS INSTITUTION OF OCEANOGRAPHY IGPP, 0225  
9500 GILMAN DRIVE  
LA JOLLA, CA 92093-0225

ROBERT BLANDFORD  
AFTAC  
1300 N. 17TH STREET  
SUITE 1450  
ARLINGTON, VA 22209-2308

STEVEN BRATT  
NTPO  
1901 N. MOORE STREET, SUITE 609  
ARLINGTON, VA 22209

RHETT BUTLER  
IRIS  
1200 NEW YORK AVE., NW  
SUITE 800  
WASHINGTON, DC 20005

LESLIE A. CASEY  
DOE  
1000 INDEPENDENCE AVE. SW  
NN-20  
WASHINGTON, DC 20585-0420

CATHERINE DE GROOT-HEDLIN  
UNIVERSITY OF CALIFORNIA, SAN DIEGO  
INSTITUTE OF GEOPHYSICS AND PLANETARY PHYSICS  
8604 LA JOLLA SHORES DRIVE  
SAN DIEGO, CA 92093

STANLEY DICKINSON  
AFOSR  
110 DUNCAN AVENUE, SUITE B115  
BOLLING AFB  
WASHINGTON, D.C. 20332-001

SEAN DORAN  
ACIS  
DCI/ACIS  
WASHINGTON , DC 20505

DIANE I. DOSER  
DEPARTMENT OF GEOLOGICAL SCIENCES  
THE UNIVERSITY OF TEXAS AT EL PASO  
EL PASO, TX 79968

RICHARD J. FANTEL  
BUREAU OF MINES  
DEPT OF INTERIOR, BLDG 20  
DENVER FEDERAL CENTER  
DENVER, CO 80225

JOHN FILSON  
ACIS/TMG/NTT  
ROOM 6T11 NHB  
WASHINGTON, DC 20505

MARK D. FISK  
MISSION RESEARCH CORPORATION  
735 STATE STREET  
P.O. DRAWER 719  
SANTA BARBARA, CA 93102-0719

LORI GRANT  
MULTIMAX, INC.  
311C FOREST AVE. SUITE 3  
PACIFIC GROVE, CA 93950

I. N. GUPTA  
MULTIMAX, INC.  
1441 MCCORMICK DRIVE  
LARGO, MD 20774

JAMES HAYES  
NSF  
4201 WILSON BLVD., ROOM 785  
ARLINGTON, VA 22230

MICHAEL HEDLIN  
UNIVERSITY OF CALIFORNIA, SAN DIEGO  
SCRIPPS INSTITUTION OF OCEANOGRAPHY IGPP, 0225  
9500 GILMAN DRIVE  
LA JOLLA, CA 92093-0225

EUGENE HERRIN  
SOUTHERN METHODIST UNIVERSITY  
DEPARTMENT OF GEOLOGICAL SCIENCES  
DALLAS, TX 75275-0395

VINDELL HSU  
HQ/AFTAC/TTR  
1030 S. HIGHWAY A1A  
PATRICK AFB, FL 32925-3002

RONG-SONG JIH  
PHILLIPS LABORATORY  
EARTH SCIENCES DIVISION  
29 RANDOLPH ROAD  
HANSOM AFB, MA 01731-3010

LAWRENCE LIVERMORE NATIONAL LABORATORY  
ATTN: TECHNICAL STAFF (PLS ROUTE)  
PO BOX 808, MS L-200  
LIVERMORE, CA 94551

LAWRENCE LIVERMORE NATIONAL LABORATORY  
ATTN: TECHNICAL STAFF (PLS ROUTE)  
PO BOX 808, MS L-221  
LIVERMORE, CA 94551

ROBERT GEIL  
DOE  
PALAIS DES NATIONS, RM D615  
GENEVA 10, SWITZERLAND

HENRY GRAY  
SMU STATISTICS DEPARTMENT  
P.O. BOX 750302  
DALLAS, TX 75275-0302

DAVID HARKRIDER  
PHILLIPS LABORATORY  
EARTH SCIENCES DIVISION  
29 RANDOLPH ROAD  
HANSOM AFB, MA 01731-3010

THOMAS HEARN  
NEW MEXICO STATE UNIVERSITY  
DEPARTMENT OF PHYSICS  
LAS CRUCES, NM 88003

DONALD HELMBERGER  
CALIFORNIA INSTITUTE OF TECHNOLOGY  
DIVISION OF GEOLOGICAL & PLANETARY SCIENCES  
SEISMOLOGICAL LABORATORY  
PASADENA, CA 91125

ROBERT HERRMANN  
ST. LOUIS UNIVERSITY  
DEPARTMENT OF EARTH & ATMOSPHERIC SCIENCES  
3507 LACLEDE AVENUE  
ST. LOUIS, MO 63103

ANTHONY IANNACCHIONE  
BUREAU OF MINES  
COCHRANE MILL ROAD  
PO BOX 18070  
PITTSBURGH, PA 15236-9986

THOMAS JORDAN  
MASSACHUSETTS INSTITUTE OF TECHNOLOGY  
EARTH, ATMOSPHERIC & PLANETARY SCIENCES  
77 MASSACHUSETTS AVENUE, 54-918  
CAMBRIDGE, MA 02139

LAWRENCE LIVERMORE NATIONAL LABORATORY  
ATTN: TECHNICAL STAFF (PLS ROUTE)  
PO BOX 808, MS L-207  
LIVERMORE, CA 94551

LAWRENCE LIVERMORE NATIONAL LABORATORY  
ATTN: TECHNICAL STAFF (PLS ROUTE)  
LLNL  
PO BOX 808, MS L-175  
LIVERMORE, CA 94551

LAWRENCE LIVERMORE NATIONAL LABORATORY  
ATTN: TECHNICAL STAFF (PLS ROUTE)  
PO BOX 808, MS L-208  
LIVERMORE, CA 94551

LAWRENCE LIVERMORE NATIONAL LABORATORY  
ATTN: TECHNICAL STAFF (PLS ROUTE)  
PO BOX 808, MS L-195  
LIVERMORE, CA 94551

THORNE LAY  
UNIVERSITY OF CALIFORNIA, SANTA CRUZ  
EARTH SCIENCES DEPARTMENT  
EARTH & MARINE SCIENCE BUILDING  
SANTA CRUZ, CA 95064

DONALD A. LINGER  
DNA  
6801 TELEGRAPH ROAD  
ALEXANDRIA, VA 22310

LOS ALAMOS NATIONAL LABORATORY  
ATTN: TECHNICAL STAFF (PLS ROUTE)  
PO BOX 1663, MS F665  
LOS ALAMOS, NM 87545

LOS ALAMOS NATIONAL LABORATORY  
ATTN: TECHNICAL STAFF (PLS ROUTE)  
PO BOX 1663, MS C335  
LOS ALAMOS, NM 87545

KEITH MCCLAUGHLIN  
MAXWELL TECHNOLOGIES  
P.O. BOX 23558  
SAN DIEGO, CA 92123

RICHARD MORROW  
USACDA/TVI  
320 21ST STREET, N.W.  
WASHINGTON, DC 20451

JAMES NI  
NEW MEXICO STATE UNIVERSITY  
DEPARTMENT OF PHYSICS  
LAS CRUCES, NM 88003

PACIFIC NORTHWEST NATIONAL LABORATORY  
ATTN: TECHNICAL STAFF (PLS ROUTE)  
PO BOX 999, MS K6-48  
RICHLAND, WA 99352

LAWRENCE LIVERMORE NATIONAL LABORATORY  
ATTN: TECHNICAL STAFF (PLS ROUTE)  
PO BOX 808, MS L-202  
LIVERMORE, CA 94551

LAWRENCE LIVERMORE NATIONAL LABORATORY  
ATTN: TECHNICAL STAFF (PLS ROUTE)  
PO BOX 808, MS L-205  
LIVERMORE, CA 94551

ANATOLI L. LEVSHIN  
DEPARTMENT OF PHYSICS  
UNIVERSITY OF COLORADO  
CAMPUS BOX 390  
BOULDER, CO 80309-0309

LOS ALAMOS NATIONAL LABORATORY  
ATTN: TECHNICAL STAFF (PLS ROUTE)  
PO BOX 1663, MS F659  
LOS ALAMOS, NM 87545

LOS ALAMOS NATIONAL LABORATORY  
ATTN: TECHNICAL STAFF (PLS ROUTE)  
PO BOX 1663, MS D460  
LOS ALAMOS, NM 87545

GARY MCCARTOR  
SOUTHERN METHODIST UNIVERSITY  
DEPARTMENT OF PHYSICS  
DALLAS, TX 75275-0395

BRIAN MITCHELL  
DEPARTMENT OF EARTH & ATMOSPHERIC SCIENCES  
ST. LOUIS UNIVERSITY  
3507 LACLEDE AVENUE  
ST. LOUIS, MO 63103

JOHN MURPHY  
MAXWELL TECHNOLOGIES  
11800 SUNRISE VALLEY DRIVE SUITE 1212  
RESTON, VA 22091

JOHN ORCUTT  
INSTITUTE OF GEOPHYSICS AND PLANETARY PHYSICS  
UNIVERSITY OF CALIFORNIA, SAN DIEGO  
LA JOLLA, CA 92093

PACIFIC NORTHWEST NATIONAL LABORATORY  
ATTN: TECHNICAL STAFF (PLS ROUTE)  
PO BOX 999, MS K7-34  
RICHLAND, WA 99352

PACIFIC NORTHWEST NATIONAL LABORATORY  
ATTN: TECHNICAL STAFF (PLS ROUTE)  
PO BOX 999, MS K6-40  
RICHLAND, WA 99352

PACIFIC NORTHWEST NATIONAL LABORATORY  
ATTN: TECHNICAL STAFF (PLS ROUTE)  
PO BOX 999, MS K5-12  
RICHLAND, WA 99352

KEITH PRIESTLEY  
DEPARTMENT OF EARTH SCIENCES  
UNIVERSITY OF CAMBRIDGE  
MADINGLEY RISE, MADINGLEY ROAD  
CAMBRIDGE, CB3 0EZ UK

PAUL RICHARDS  
COLUMBIA UNIVERSITY  
LAMONT-DOHERTY EARTH OBSERVATORY  
PALISADES, NY 10964

CHANDAN SAIKIA  
WOODWARD-CLYDE FEDERAL SERVICES  
566 EL DORADO ST., SUITE 100  
PASADENA, CA 91101-2560

SANDIA NATIONAL LABORATORY  
ATTN: TECHNICAL STAFF (PLS ROUTE)  
DEPT. 5791  
MS 0567, PO BOX 5800  
ALBUQUERQUE, NM 87185-0567

SANDIA NATIONAL LABORATORY  
ATTN: TECHNICAL STAFF (PLS ROUTE)  
DEPT. 5704  
MS 0655, PO BOX 5800  
ALBUQUERQUE, NM 87185-0655

THOMAS SERENO JR.  
SCIENCE APPLICATIONS INTERNATIONAL  
CORPORATION  
10260 CAMPUS POINT DRIVE  
SAN DIEGO, CA 92121

ROBERT SHUMWAY  
410 MRAK HALL  
DIVISION OF STATISTICS  
UNIVERSITY OF CALIFORNIA  
DAVIS, CA 95616-8671

DAVID SIMPSON  
IRIS  
1200 NEW YORK AVE., NW  
SUITE 800  
WASHINGTON, DC 20005

PACIFIC NORTHWEST NATIONAL LABORATORY  
ATTN: TECHNICAL STAFF (PLS ROUTE)  
PO BOX 999, MS K6-84  
RICHLAND, WA 99352

FRANK PILOTTE  
HQ/AFTAC/TT  
1030 S. HIGHWAY A1A  
PATRICK AFB, FL 32925-3002

JAY PULLI  
RADIX SYSTEMS, INC.  
6 TAFT COURT  
ROCKVILLE, MD 20850

DAVID RUSSELL  
HQ AFTAC/TTR  
1030 SOUTH HIGHWAY A1A  
PATRICK AFB, FL 32925-3002

SANDIA NATIONAL LABORATORY  
ATTN: TECHNICAL STAFF (PLS ROUTE)  
DEPT. 5704  
MS 0979, PO BOX 5800  
ALBUQUERQUE, NM 87185-0979

SANDIA NATIONAL LABORATORY  
ATTN: TECHNICAL STAFF (PLS ROUTE)  
DEPT. 9311  
MS 1159, PO BOX 5800  
ALBUQUERQUE, NM 87185-1159

SANDIA NATIONAL LABORATORY  
ATTN: TECHNICAL STAFF (PLS ROUTE)  
DEPT. 5736  
MS 0655, PO BOX 5800  
ALBUQUERQUE, NM 87185-0655

AVI SHAPIRA  
SEISMOLOGY DIVISION  
THE INSTITUTE FOR PETROLEUM RESEARCH AND  
GEOPHYSICS  
P.O.B. 2286, NOLON 58122 ISRAEL

MATTHEW SIBOL  
ENSCO, INC.  
445 PINEDA COURT  
MELBOURNE, FL 32940

JEFFRY STEVENS  
MAXWELL TECHNOLOGIES  
P.O. BOX 23558  
SAN DIEGO, CA 92123

BRIAN SULLIVAN  
BOSTON COLLEGE  
INSTITUTE FOR SPACE RESEARCH  
140 COMMONWEALTH AVENUE  
CHESTNUT HILL, MA 02167

NAFI TOKSOZ  
EARTH RESOURCES LABORATORY, M.I.T.  
42 CARLTON STREET, E34-440  
CAMBRIDGE, MA 02142

GREG VAN DER VINK  
IRIS  
1200 NEW YORK AVE., NW  
SUITE 800  
WASHINGTON, DC 20005

TERRY WALLACE  
UNIVERSITY OF ARIZONA  
DEPARTMENT OF GEOSCIENCES  
BUILDING #77  
TUCSON, AZ 85721

JAMES WHITCOMB  
NSF  
NSF/ISC OPERATIONS/EAR-785  
4201 WILSON BLVD., ROOM 785  
ARLINGTON, VA 22230

JIAKANG XIE  
COLUMBIA UNIVERSITY  
LAMONT DOHERTY EARTH OBSERVATORY  
ROUTE 9W  
PALISADES, NY 10964

OFFICE OF THE SECRETARY OF DEFENSE  
DDR&E  
WASHINGTON, DC 20330

TACTEC  
BATTELLE MEMORIAL INSTITUTE  
505 KING AVENUE  
COLUMBUS, OH 43201 (FINAL REPORT)

PHILLIPS LABORATORY  
ATTN: GPE  
29 RANDOLPH ROAD  
HANSCOM AFB, MA 01731-3010

PHILLIPS LABORATORY  
ATTN: PL/SUL  
3550 ABERDEEN AVE SE  
KIRTLAND, NM 87117-5776 (2 COPIES)

DAVID THOMAS  
ISEE  
29100 AURORA ROAD  
CLEVELAND, OH 44139

LAWRENCE TURNBULL  
ACIS  
DCI/ACIS  
WASHINGTON, DC 20505

FRANK VERNON  
UNIVERSITY OF CALIFORNIA, SAN DIEGO  
SCRIPPS INSTITUTION OF OCEANOGRAPHY IGPP, 0225  
9500 GILMAN DRIVE  
LA JOLLA, CA 92093-0225

DANIEL WEILL  
NSF  
EAR-785  
4201 WILSON BLVD., ROOM 785  
ARLINGTON, VA 22230

RU SHAN WU  
UNIVERSITY OF CALIFORNIA SANTA CRUZ  
EARTH SCIENCES DEPT.  
1156 HIGH STREET  
SANTA CRUZ, CA 95064

JAMES E. ZOLLWEG  
BOISE STATE UNIVERSITY  
GEOSCIENCES DEPT.  
1910 UNIVERSITY DRIVE  
BOISE, ID 83725

DEFENSE TECHNICAL INFORMATION CENTER  
8725 JOHN J. KINGMAN ROAD  
FT BELVOIR, VA 22060-6218 (2 COPIES)

PHILLIPS LABORATORY  
ATTN: XPG  
29 RANDOLPH ROAD  
HANSCOM AFB, MA 01731-3010

PHILLIPS LABORATORY  
ATTN: TSML  
5 WRIGHT STREET  
HANSCOM AFB, MA 01731-3004